Atmospheric
Chemistry
and Physics
Discussions

Drivers of diel and regional variations of halocarbon emissions from the tropical North East Atlantic

H. Hepach[1], B. Quack[1], F. Ziska[1], S. Fuhlbrügge[1], E. L. Atlas[2], I. Peeken[3,4], K. Krüger[1], and D. W. R. Wallace[1,*]

[1]GEOMAR Helmholtz-Zentrum für Ozeanforschung Kiel, Germany
[2]Rosenstiel School of Marine and Atmospheric Science (RSMAS), University of Miami, USA
[3]Alfred-Wegener-Institut für Polar und Meeresforschung (AWI), Bremerhaven, Germany
[4]MARUM – Center for Marine Environmental Sciences, University Bremen, Bremen, Germany
[*]now at: Department of Oceanography, Dalhousie University, Halifax, Canada

Correspondence to: H. Hepach (hhepach@geomar.de)

Drivers of diel and regional variations

H. Hepach et al.

Title Page

Abstract	Introduction
Conclusions	References
Tables	Figures

◄◄ ►►

◄ ►

Back Close

Full Screen / Esc

Printer-friendly Version

Interactive Discussion

Abstract

Methyl iodide (CH_3I), bromoform ($CHBr_3$) and dibromomethane (CH_2Br_2), which are produced naturally in the oceans, take part in ozone chemistry both in the troposphere and the stratosphere. The significance of oceanic upwelling regions for emissions of these trace gases in the global context is still uncertain although they have been identified as important source regions. To better quantify the role of upwelling areas in current and future climate, this paper analyzes major factors that influenced halocarbon emissions from the tropical North East Atlantic including the Mauritanian upwelling during the DRIVE expedition. Diel and regional variability of oceanic and atmospheric CH_3I, $CHBr_3$ and CH_2Br_2 was determined along with biological and meteorological parameters at six 24 h-stations. Low oceanic concentrations of CH_3I from 0.1–5.4 $pmol L^{-1}$ were equally distributed throughout the investigation area. $CHBr_3$ of 1.0–42.4 $pmol L^{-1}$ and CH_2Br_2 of 1.0–9.4 $pmol L^{-1}$ were measured with maximum concentrations close to the Mauritanian coast. Atmospheric mixing rations of CH_3I of up to 3.3, $CHBr_3$ to 8.9 and CH_2Br_2 to 3.1 ppt above the upwelling and 1.8, 12.8, respectively 2.2 ppt at a Cape Verdean coast were detected during the campaign. While diel variability in CH_3I emissions could be mainly ascribed to oceanic non-biological production, no main driver was identified for its emissions in the entire study region. In contrast, oceanic bromocarbons resulted from biogenic sources which were identified as regional drivers of their sea-to-air fluxes. The diel impact of wind speed on bromocarbon emissions increased with decreasing distance to the coast. The height of the marine atmospheric boundary layer (MABL) was determined as an additional factor influencing halocarbon emissions. Oceanic and atmospheric halocarbons correlated well in the study region and in combination with high oceanic CH_3I, $CHBr_3$ and CH_2Br_2 concentrations, local hot spots of atmospheric halocarbons could solely be explained by marine sources. This conclusion is in contrast with previous studies that hypothesized the occurrence of elevated atmospheric halocarbons over the eastern tropical Atlantic mainly originating from the West-African continent.

1 Introduction

Volatile halogenated hydrocarbons (halocarbons) occur naturally in the oceans from where they are emitted into the atmosphere. Bromine and iodine atoms released from these compounds by photolysis and oxidation can take part in catalytic ozone destroying cycles in both the troposphere and stratosphere (McGivern et al., 2000; Salawitch et al., 2005; Montzka and Reimann, 2011) with iodine also participating in aerosol formation (O'Dowd et al., 2002). While the brominated trace gases bromoform ($CHBr_3$) and dibromomethane (CH_2Br_2) represent the largest contributors to atmospheric organic bromine from the ocean to the atmosphere (Hossaini et al., 2012a), methyl iodide (CH_3I), originating mostly from marine sources, is the most abundant organoiodine in the atmosphere (Saiz-Lopez et al., 2012).

Elevated halocarbon concentrations, particularly of $CHBr_3$ and CH_2Br_2, are generally associated with marine biological active areas like coastal regions where macro algae are thought to be the most dominant sources (Carpenter and Liss, 2000; Laturnus, 2001). Phytoplankton produces these trace gases as well and especially upwelling regions where cold, nutrient rich water is brought up to the sea surface contains large amounts of these compounds (Tokarczyk and Moore, 1994; Quack et al., 2004). Other production pathways than biological production have been proposed such as photochemistry that could be of high significance for the marine formation of iodinated organic trace gases, e.g. CH_3I. Hence, its distribution in the ocean may depend on physical parameters including insolation and sea surface temperature (SST) (Moore and Groszko, 1999; Richter and Wallace, 2004; Yokouchi et al., 2008). There are still large uncertainties regarding the sources and drivers of marine halocarbon distributions and emissions, while even less is known about their diel variability.

The tropical regions represent the largest contributors to global emission budgets of CH_3I, $CHBr_3$ and CH_2Br_2 (Ziska et al., 2013). Once they are produced and emitted from the tropical oceans, halocarbons and their degradation products can be carried in significant quantities into the stratosphere (Solomon et al., 1994; Hossaini et al., 2010;

Aschmann et al., 2011; Montzka and Reimann, 2011; Tegtmeier et al., 2013), since deep tropical convection can lift surface air very rapidly into the tropical tropopause layer (Tegtmeier et al., 2012). Considerable changes in future inorganic bromine in the tropical troposphere (Pyle et al., 2007) and to the stratosphere (Hossaini et al., 2012b)
5 from biogenic halocarbon emissions due to strengthening of convection were projected by chemistry climate models leading to increasing importance of tropical halocarbon emissions. Coastal upwelling systems might play a crucial role in a changing climate. The tropical Mauritanian upwelling is an example for a recently intensified coastal eastern boundary upwelling (McGregor et al., 2007). Primary production could increase
10 with enhanced entrainment of nutrient rich deep water into the surface ocean leading to amplified production of halocarbons. Increasing wind speeds, caused by enhanced pressure gradients (Bakun, 1990), would also directly influence the sea-to-air fluxes of all trace gases via a faster transfer coefficient (e.g. Nightingale et al., 2000). Thus the identification of factors impacting halocarbon sea-to-air fluxes is crucial for assessing
15 possible effects of climate change on future emissions from coastal upwelling systems. Previous studies have hypothesized that elevated atmospheric mixing ratios of $CHBr_3$ and CH_2Br_2 above the Mauritanian upwelling area were mainly of continental origin, since sea-to-air fluxes of these compounds appeared not sufficient to explain the observations (Quack et al., 2007a; Carpenter et al., 2009). In contrast, the investigation
20 by Fuhlbrügge et al. (2013) revealed high atmospheric mixing ratios of CH_3I, $CHBr_3$ and CH_2Br_2 close to the coast also in air masses transported from the northern open ocean, with a significant anticorrelation between the atmospheric mixing ratios and the height of the marine atmospheric boundary layer (MABL).

This paper reports on oceanic and atmospheric halocarbon distributions and sea-
25 to-air fluxes from the DRIVE (Diurnal and RegIonal Variability of halogen Emissions) campaign of RV *Poseidon* in the eastern tropical North Atlantic ocean and the Mauritanian upwelling in June 2010. We present results from six 24 h-stations in different distances from the Mauritanian coast and from two parallel diel stations on the Cape Verde island Sao Vincente. We aim at describing and quantifying significant factors

that control the concentrations and emission fluxes of CH_3I, $CHBr_3$, and CH_2Br_2 both on a diel and a regional scale, including biological and photochemical production, wind speed, SST, and atmospheric transport. Furthermore, we examine how oceanic emissions contribute to the mixing ratios of atmospheric halocarbons taking the height of the marine atmospheric boundary layer (MABL) into account. Other meteorological constraints, e.g. wind conditions and back trajectory analysis, on atmospheric measurements during the cruise are investigated in the accompanying paper by Fuhlbrügge et al. (2013).

2 Methods

The cruise P399/2 (*Poseidon* 399 leg 2) named DRIVE (Diurnal and Regional Variability of halogen Emissions) of RV *Poseidon* took place from 31 May to 17 June in 2010 in the eastern tropical North Atlantic ocean and the Mauritanian upwelling. The ship followed a course from Las Palmas (Canary Islands, 28.1° N and 15.4° W) back to Las Palmas with a short stop at Mindelo (Sao Vicente, Cape Verde, 16.9° N and 25.0° W). The cruise track included six 24 h-stations located at 17.6° N and 24.3° W (S1), 18.0° N and 21.0° W (S2), 18.0° N and 18.0° W (S3), 18.5° N and 16.5° W (S4), 19.0° N and 16.6° W (S5), and 20.0° N and 17.3° W (S6) where the ship remained at its position for 24 h (Fig. 1). Parallel samples for dissolved halocarbons in sea water, atmospheric halocarbons and phytoplankton pigments were taken at all 24 h-stations, and additionally four radio sonde launches per 24 h-station were accomplished to determine the MABL properties. For more details on the campaign and the meteorological parameters see the cruise report by Bange et al. (2011) and the accompanying paper of Fuhlbrügge et al. (2013).

Related to the ship expedition a land-based operation took place from 3 June to 8 June 2010 at the Cape Verde Atmospheric Observatory (CVAO) on Sao Vincente close to Mindelo at 17.6° N and 24.3° W (Fig. 1) were samples of atmospheric halocarbons were taken during two days.

Drivers of diel and regional variations

H. Hepach et al.

Title Page

Abstract	Introduction
Conclusions	References
Tables	Figures

|◀ | ▶|

◀ | ▶

Back | Close

Full Screen / Esc

Printer-friendly Version

Interactive Discussion

Atmospheric halocarbon mixing ratios and meteorological conditions were also determined during a second cruise leg P399/3 from Las Palmas, Spain to Vigo, Spain and are covered in Fuhlbrügge et al. (2013). In contrast, this manuscript focuses only on results from leg P399/2. The words "whole cruise" will refer to leg 2 and "whole campaign" includes leg 2 and the land-based operation at Cape Verde.

2.1 Sampling and analysis of halocarbons in sea surface water and air

Dissolved halocarbons were sampled in 500 mL amber glass bottles from a continuously working pump from the ships moon pool at a depth of 4.4 m. This allowed for nearly hourly sampling of sea surface water at every diel station. In between 24 h-stations, the samples were taken every 3 h. The water was analyzed for halocarbons using a purge and trap system attached to a gas chromatograph with mass spectrometric detection (GC-MS). 80 mL of water were purged with a stream of helium at 30 mL min^{-1} at 70 °C in a glass chamber. The volatilized trace gases were desiccated with a Nafion$^{®}$ dryer using nitrogen as drying gas and were trapped on glass beads at -100 °C. After one hour of purging, the compounds were desorbed at 100 °C onto a deactivated capillary in liquid nitrogen as second trap. After three minutes, the sample was injected into the GC-MS, the trace gases were separated on a Rtx-VGC capillary column with a length of 60 m, a diameter of 0.25 mm and a film thickness of 1.40 µm, and were detected in single ion mode. Quantification was achieved with volumetrically prepared standards in methanol. Precision for these measurements lay within 16 % for CH_3I, and 6 % for $CHBr_3$ and CH_2Br_2 determined from duplicates.

Air samples were taken hourly at the diel stations, being pumped into stainless steel canisters on the compass deck at a height of 13.7 m with a metal bellows pump. Samples were analyzed within a month at the Rosenstiel School of Marine and Atmospheric Science in Miami with a precision of approximately 5 % using GC-MS (Schauffler et al., 1999). Additionally, air samples were taken at CVAO on an hourly basis parallel to the first two diel stations of the ship. Samples were taken according to the method onboard the RV *Poseidon* in approximately 3 m height above ground and then analyzed along

with the other canisters collected during the cruise. Oceanic and atmospheric measurements were intercalibrated against whole air working-standards obtained from the NOAA Global Monitoring Division (Boulder, USA).

2.2 Phytoplankton pigment analysis and flow cytometry

Samples for pigment analysis were taken approximately every 2 h at every diel station. 1 L of sea surface water from the ships' underway pump system was filtered through 25 mm Whatman GF/F filters and stored at −80 °C until analysis. Back in the lab, phytoplankton pigments were analyzed according to Tran et al. (2013) using a waters high-performance liquid chromatography (HPLC) system at the Alfred Wegener Institute for Polar and Marine Research Bremerhaven (AWI). The 28 marker pigments for which samples were analyzed include various chlorophyll type pigments such as chlorophyll $c1$, $c2$ and $c3$, divinyl chlorophyll b, chlorophyll b, divinyl chlorophyll a, chlorophyll a (Chl a), and phaeophytin a. The following carotenoids were detected: peridin, predinin derivative, 19-butanoyloxyfucoxanthin, fucoxanthin, neoxanthin, 19-hexanoyloxyfucoxanthin, violaxanthin, astaxanthin, prasinoxanthin, diadinoxanthin, alloxanthin, diatoxanthin, anthreaxanthin, zeaxanthin, lutein, α-carotene, and β-carotene. The marker pigments are indicative for different phytoplankton groups.

For flow cytometry, 4 mL of water from the underway pump system were preserved with glutaraldehyde with a final concentration of 0.1 %, shock frozen in liquid nitrogen and stored at −80 °C. Flow cytometry samples were also analyzed at the AWI according to Taylor et al. (2011).

2.3 Calculation of sea-to-air fluxes and saturation anomaly

Sea-to-air fluxes (F) of CH_3I, $CHBr_3$ and CH_2Br_2 were calculated using the air–sea gas exchange parameterization of Nightingale et al. (2000). Schmidt number (Sc) corrections for the compound specific transfer coefficients k_w derived with the transfer

coefficient k_{CO_2} of CO_2 as reported by Quack and Wallace (2003) were applied.

$$\frac{k_w}{k_{CO_2}} = \frac{Sc}{660}^{-\frac{1}{2}} \tag{1}$$

The air–sea concentration gradient was derived from all simultaneous water (c_w) and air (c_{atm}) measurements calculated with the Henry's law constants H of Moore and co-workers (Moore et al., 1995a, b) to obtain the theoretical equilibrium concentration c_{atm}/H.

$$F = k_w \cdot \left(c_w - \frac{c_{atm}}{H} \right) \tag{2}$$

The saturation anomaly S was calculated from the concentration gradient as the percentage of the equilibrium concentration.

$$S = \left(\left(c_w - \frac{c_{atm}}{H} \right) \cdot 100 \right) \cdot \left(\frac{c_{atm}}{H} \right)^{-1} \tag{3}$$

Water temperature and salinity were continuously recorded using the ships' thermosalinograph. Air pressure and wind speed were determined by sensors on the compass deck and in 25.5 m height, respectively. 10 min averages of these four parameters were included in the calculations, and wind speed was corrected to 10 m values.

3 Hydrography and environmental parameters during DRIVE

High SST values between 23.0 and 24.7 °C and high salinities from 36.4 to 36.7 observed at S1 and S2 close to Cape Verde (Figs. 1 and 2a, Table 1) were consistent with tropical surface water characteristics (Tsuchiya et al., 1992). Low Chl *a* concentrations between 0.00 and 0.43 µg L^{-1} were a sign of low primary production there. Stations S1

Drivers of diel and regional variations

H. Hepach et al.

Title Page

Abstract	Introduction
Conclusions	References
Tables	Figures

◀ ▶|

◀ ▶

Back | Close

Full Screen / Esc

Printer-friendly Version

Interactive Discussion

and S2 are hence defined as open ocean. Wind speed had the lowest mean of the whole cruise at S1 with $4.6\,\mathrm{m\,s^{-1}}$ and was highest at S2 with a mean of $11.0\,\mathrm{m\,s^{-1}}$. The MABL height in this region determined by Fuhlbrügge et al. (2013) ranged between 400 and 1100 m (Table 1). With decreasing distance to the Mauritanian coast, starting at S3, a decrease in SST and salinity and an increase in Chl a concentrations were observed. This is a sign of the North West African upwelling system on the African shelf as part of the wind-driven Canary Current extending from $30°$ N to $10°$ N (Fedoseev, 1970). South Atlantic Central Water (SACW), characterized as a straight T-S curve between $5\,°C$ and 34.3 and $20\,°C$ and 36.0 (Tomczak and Godfrey, 2005), is transported to the Mauritanian coast by a poleward directed undercurrent. Between $12°$ N and $20°$ N upwelling of the cold nutrient rich SACW takes place from late fall to late spring (Minas et al., 1982; Tomczak, 1982; Hagen, 2001) after which the upwelling starts to cease due to changing atmospheric conditions induced by the shift of the Intertropical Convergence Zone (Mittelstaedt, 1982). The beginning ceasing of the upwelling could be observed during DRIVE at stations S3–S6, which are defined as upwelling and coastal stations (further on called coastal stations). The lowest SST with $18.4\,°C$ as well as the highest daily mean Chl a concentration of $4.80\,\mathrm{\mu g\,L^{-1}}$ were found at the northernmost station (S6), while the overall maximum Chl a concentration of $8.12\,\mathrm{\mu g\,L^{-1}}$ was observed at S5. MABL heights generally ranged between surface and 400 m at S3–S6, while wind speeds varied between 3.9 (S3) and $14.2\,\mathrm{m\,s^{-1}}$ (S6). At S5, the lowest MABL heights (close to the surface) together with the highest relative standard deviation (further on referred to as variability) in wind speed with a mean of $8.9\,\mathrm{m\,s^{-1}}$ and a variability of 27 % was observed at one station in the course of 24 h (Table 1).

4 Results

4.1 Methyl iodide (CH_3I)

4.1.1 Regional distribution

Oceanic CH_3I was with 2.4 pmol L^{-1} on average higher at the open ocean stations S1 and S2 than at coastal stations S3–S6 with 1.8 pmol L^{-1} (Fig. 2b, Table 2). While maximum mean (min–max) oceanic CH_3I of 3.0 (1.7–5.4) pmol L^{-1} was observed at S1, S3 showed the lowest mean CH_3I concentrations of 1.2 (0.2–2.1) pmol L^{-1} during 24 h. In total, the mean regional variability of CH_3I was the lowest of all three halocarbons with a relative standard deviation of 56 %. Correlations to neither phytoplankton pigments nor to picoplankton abundances were found for CH_3I in sea surface water (Table 3).

Atmospheric CH_3I with an overall mean of 1.3 (0.6–3.3) ppt revealed a different distribution in comparison to oceanic CH_3I (Fig. 2a). It was generally lower above the open ocean with 0.9 (0.6–1.3) ppt on average and increased towards the coast with a mean (range) of 1.6 (0.9–3.3) ppt (see also Fuhlbrügge et al., 2013). In total, atmospheric CH_3I had a lower regional variability of 44 % than oceanic CH_3I.

4.1.2 Diel variations

Of all three halocarbons, oceanic CH_3I showed the largest diel variability which was also larger than its regional variability. The lowest and the highest mean variability during 24 h were found at S1 with 29 % and with 62 % at S2, respectively. At the coastal stations oceanic CH_3I varied between 37 % (S6) and 60 % (S4). While at four stations maxima of CH_3I in the surface water were found in the morning hours, elevations in the afternoon were observed at open ocean station S2 and coastal station S6. Hence, no overall diurnal cycle could be detected.

Low relative diel variability between 9 % (S2) and 11 % (S1) was observed in atmospheric CH_3I above the open ocean. The variability at CVAO at the same time ranged

Drivers of diel and regional variations

H. Hepach et al.

Title Page

Abstract	Introduction
Conclusions	References
Tables	Figures

◄ | ►

◄ | ►

Back | Close

Full Screen / Esc

Printer-friendly Version

Interactive Discussion

between 9 % (4 June, parallel to S1) and 14 % (6 and 7 June, parallel to S2) (Fig. 3a, Table 2) with mean mixing ratios of 1.2 ppt (0.7 ppt at 4 June – 1.8 ppt at 6 June). At the coastal stations S3–S6, diel variability of 7 (S3)–33 % (S4) was observed. The high mean atmospheric variability at S4 coincides with the largest oceanic variability. Similarly to oceanic concentrations of CH_3I, there is no overall diurnal cycle in atmospheric mixing ratios. Maxima and minima occurred in both day and night hours.

4.1.3   Saturation anomaly, sea–air concentration gradient and sea-to-air fluxes

Saturation anomalies (Fig. 4), sea–air concentration gradient (Fig. 5b) as well as sea-to-air fluxes (Fig. 5c) were calculated according to Eqs.(1)–(3) (Table 2). To constrain the atmospheric influence on the concentration gradient, and eventually on the sea-to-air fluxes, the fraction of the equilibrium concentration c_{atm}/H of the oceanic concentration c_w was calculated (Fig. 6a). This is the relative reduction of the concentration gradient through the atmospheric mixing ratios, and consequently of the sea-to-air flux (compare Eq. 2) which will be referred to as "flux reducing effect" further on.

Of the three halocarbons the highest saturation anomalies and the lowest concentration gradient $c_w - c_{atm}/H$ were calculated for CH_3I with means of 931 (−66–4597) % (Fig. 4a, Table 2) and 1.7 (−0.3–5.3) pmol L^{-1} (Fig. 5b) for the whole cruise. Both were consistent with the oceanic distribution: they were highest in the open ocean with maxima at S1 where however no exceptionally high emissions of this compound were calculated because of the prevailing low wind speeds during that time (Fig. 5c). The open ocean was generally highly supersaturated in CH_3I with anomalies of 1715 % on average and decreasing towards the coastal stations with a coastal mean of 522 %. The reducing effect of atmospheric CH_3I was low. The concentration gradient, and therewith the sea-to-air flux, was usually reduced by less than 50 %. One exception was S5 where low oceanic CH_3I coincided with high atmospheric mixing ratios, and the flux reducing effect reached 300 %. Mainly positive fluxes could be observed with mean sea-to-air fluxes of CH_3I of 254 pmol m^{-2} h^{-1} for the whole cruise (−65 at coastal sta-

tion S5 to 942 pmol m^{-2} h^{-1} at open ocean station S2) (Fig. 5c, Table 2). In agreement with both saturation anomaly and concentration gradient, a slightly higher mean of 268 pmol m^{-2} h^{-1} was calculated for the open ocean stations S1 and S2 in comparison to the mean coastal flux of 246 pmol m^{-2} h^{-1} for S3–S6.

4.1.4 Impact of oceanic CH$_3$I and wind speed on fluxes

For the whole cruise, the sea-to-air flux of CH$_3$I showed significant but low regional correlations with sea surface concentrations ($R^2 = 0.37$) and wind speed ($R^2 = 0.24$) (Fig. 7a and d, Table 4). Considering each station individually, high significant correlations of CH$_3$I in sea surface water to sea-to-air flux were found at open ocean station S2 and at all coastal stations with R^2 ranging between 0.57 and 0.91. Significant correlations of wind speed to sea-to-air flux of CH$_3$I could only be detected at coastal station S3 and at open ocean station S1 ($R^2 = 0.24$ and 0.76).

4.2 Bromoform (CHBr$_3$) and dibromomethane (CH$_2$Br$_2$)

4.2.1 Regional distribution

CHBr$_3$ and CH$_2$Br$_2$ in water showed analogous patterns (Fig. 2c and d, Table 2). Both were lower in the open ocean (S1 and S2) with means of 2.3 (1.0–3.8) pmol L^{-1} for CHBr$_3$ and 1.6 (1.0–2.2) pmol L^{-1} for CH$_2$Br$_2$ with minimum concentrations at S1. Both compounds had higher coastal concentrations of 18.3 (8.1–42.4) pmol L^{-1} for CHBr$_3$ and 5.8 (3.1–9.4) pmol L^{-1} for CH$_2$Br$_2$ with maxima at S5 and a much more pronounced increase in oceanic CHBr$_3$ than in CH$_2$Br$_2$. CHBr$_3$ and CH$_2$Br$_2$ in sea surface water demonstrated much higher relative regional variability of 78 % (CHBr$_3$) and 59 % (CH$_2$Br$_2$) than oceanic CH$_3$I.

Atmospheric CHBr$_3$ and CH$_2$Br$_2$ increased towards the upwelling and coast similarly to their oceanic counterparts (Fig. 2c and d, as well as Table 2). Atmospheric CHBr$_3$

Drivers of diel and regional variations

H. Hepach et al.

Title Page

Abstract	Introduction
Conclusions	References
Tables	Figures

|◀ | ▶|

◀ | ▶

Back | Close

Full Screen / Esc

Printer-friendly Version

Interactive Discussion

showed with 56 % the highest mean regional variability of the three halocarbons, while atmospheric CH_2Br_2 had the lowest regional variability of 33 %.

4.2.2 Diel variations

Diel variations of both $CHBr_3$ and CH_2Br_2 in sea surface water were generally lower than their regional variations. While the variability of $CHBr_3$ only ranged between 14 % with a mean of $1.2\,pmol\,L^{-1}$ (S1) and 19 % with a mean of $3.0\,pmol\,L^{-1}$ (S2) in the open ocean, the variability of CH_2Br_2 was even lower with 7 % (S1) and 9 % (S2) and mean concentrations of $1.2–1.9\,pmol\,L^{-1}$. At most of the coastal stations $CHBr_3$ and CH_2Br_2 revealed similar distributions throughout 24 h with maxima in the evening and night hours with the exception of S5 were maxima of $42.4\,pmol\,L^{-1}$ ($CHBr_3$) and $9.4\,pmol\,L^{-1}$ (CH_2Br_2) were found in the morning hours. The highest diel variation of 23 % was found at coastal station S3 for oceanic $CHBr_3$, while CH_2Br_2 was generally less variable ranging from 4 (S5) to 10 % (S4).

Atmospheric mixing ratios of $CHBr_3$ and CH_2Br_2 were low in the open ocean with relative standard deviations of 13–19 % ($CHBr_3$) and 5–9 % (CH_2Br_2). Atmospheric bromocarbons and their mean variability were generally higher at CVAO with means (variability) for $CHBr_3$, respectively CH_2Br_2 of 6.7 ppt (43 %) and 1.4 ppt (16 %) on 4 June to 6.8 ppt (35 %) and 1.5 ppt (14 %) on 6 and 7 June (Fig. 3b and c, Table 2). The highest atmospheric $CHBr_3$ during the whole campaign of 12.8 ppt was measured at CVAO on 7 June. The diel variability of atmospheric $CHBr_3$ at the coastal stations S3–S6 was generally lower than what was observed above the open ocean with 7 (S3)–14 % (S4). The diel variability of atmospheric CH_2Br_2 at the coast was similar to the open ocean with 5 (S6)–10 % (S4). Atmospheric $CHBr_3$ and CH_2Br_2 showed no overall diurnal cycles above neither open ocean nor coastal stations with maxima during both day and night hours.

4.2.3 Correlations of $CHBr_3$ and CH_2Br_2 with phytoplankton pigments

The correlation coefficient R^2 of 0.38 and 0.49 for surface Chl *a* to $CHBr_3$ respectively CH_2Br_2 for the entire investigated region was significant at the 95 % level (Table 3, Fig. 2a). Significant but low correlations were found to *Prochlorococcus*. Additionally,
5 multiple linear regressions (MLR) of brominated halocarbons to all phytoplankton pigments except for Chl *a* were carried out for the whole cruise. All pigment data related to $CHBr_3$ or CH_2Br_2 with $p < 0.05$ was regarded as significant. The six pigments chlorophyll *b*, chlorophyll *c*3, fucoxanthin, diatoxanthin, pyrophaeophorbide *a* and zeaxanthin were found to describe the regional distribution of $CHBr_3$ best (Fig. 2e, Table 3). Chloro-
10 phyll *b*, fucoxanthin, α-carotene (negatively correlated) and alloxanthin were important for CH_2Br_2 in the order of explanatory power.

4.2.4 Saturation anomaly, sea–air concentration gradients and sea-to-air fluxes

Saturation anomalies (Fig. 4), sea–air concentration gradients (Fig. 5b) and sea-to-air fluxes (Fig. 5c) were calculated according to Eqs. (1)–(3) (Table 2), and similarly
15 to CH_3I, the influence of the atmospheric mixing ratios on the concentration gradient of $CHBr_3$ and CH_2Br_2 via the equilibration concentration c_{atm}/H was determined (Fig. 6b, c).

The ocean was generally supersaturated with both $CHBr_3$ and CH_2Br_2. The overall saturation anomaly of 65 (−40–243) % for $CHBr_3$ was slightly lower than the mean of
20 CH_2Br_2 with 84 (3–204) % (Fig. 4b). Both displayed similar trends opposite to CH_3I: lower saturation anomalies of around 30 % for both compounds at the open ocean stations, followed by an increase towards the coastal stations S3–S6 with means of 83 % for $CHBr_3$ and 110 % for CH_2Br_2. Maximum saturation anomalies coincided with maximum oceanic and atmospheric bromocarbons at S5 with daily means of 148 %
25 for $CHBr_3$ and 169 % for CH_2Br_2. The concentration gradient $c_w − c_{atm}/H$ of $CHBr_3$ was the highest of all three halocarbons with a total mean of 5.8 (−1.3–30.0) pmol L^{-1}, followed by CH_2Br_2 with a mean of 2.2 (0–6.3) pmol L^{-1} and minima in the open ocean

region (Fig. 5b). The reducing effect of atmospheric $CHBr_3$ and CH_2Br_2 on the sea-to-air flux was large in the open ocean ($> 75\%$) where both compounds were close to equilibrium and decreases simultaneously with the strongly increasing concentration gradient towards the coast (Fig. 6b and c). For $CHBr_3$ and CH_2Br_2 the flux reducing effect was around 50 % at the four coastal stations (S3–S6). Sea-to-air fluxes of $CHBr_3$ and CH_2Br_2 for the whole cruise were according to the considerably larger concentration gradients on average higher than CH_3I fluxes with 787 (−273–6069) $pmol\,m^{-2}\,h^{-1}$ and 341 (2–1429) $pmol\,m^{-2}\,h^{-1}$, respectively (Fig. 5c, Table 2). Fluxes of both compounds were low in the open ocean region with means of 41 $pmol\,m^{-2}\,h^{-1}$ for $CHBr_3$ and of 66 $pmol\,m^{-2}\,h^{-1}$ for CH_2Br_2. Higher sea-to-air fluxes of $CHBr_3$ and CH_2Br_2 with means of 1171 $pmol\,m^{-2}\,h^{-1}$ and 483 $pmol\,m^{-2}\,h^{-1}$ were observed at the coastal stations S3–S6. The maximum fluxes of both compounds were found at coastal station 5.

4.2.5 Impact of oceanic $CHBr_3$ and CH_2Br_2 and wind speed on fluxes

Sea surface water concentrations of $CHBr_3$ and CH_2Br_2 correlated regionally to sea-to-air fluxes with $R^2 = 0.68$ ($CHBr_3$) and 0.71 (CH_2Br_2) for the whole cruise (Fig. 7, Table 4). Significant correlations of $CHBr_3$ fluxes with sea surface water concentrations were found at all 24 h-stations (R^2 from 0.34 to 0.78). The highest correlations of sea surface CH_2Br_2 to its sea-to-air fluxes were found at open ocean station S2 (0.64) and coastal stations S3 and S4 (0.42, 0.53). No significant correlations could be observed at coastal stations S5 and S6. In contrast, wind speed showed regionally significant but low correlations to the overall sea-to-air flux with $R^2 = 0.14$ ($CHBr_3$) and $R^2 = 0.29$ (CH_2Br_2). Considering the stations individually, $CHBr_3$ and CH_2Br_2 revealed high correlations of wind speed with sea-to-air flux at coastal stations S4–S6 with R^2 from 0.56 to 0.95.

5 Discussion

5.1 Sea-to-air fluxes of CH_3I

5.1.1 Oceanic and atmospheric CH_3I as drivers of the regional and diel variability of the concentration gradient

The ocean was highly supersaturated with CH_3I throughout most of the cruise which is underlined by the low impact of atmospheric CH_3I on its concentration gradient (Fig. 6a). Regional and diel variability in the concentration gradient was primarily a result of varying oceanic CH_3I. The oceanic measurements during DRIVE (0.1 to 5.4 pmol L^{-1}, Table 2) compare well to the measurements by Schall et al. (1997) of 0–3 pmol L^{-1} in the Atlantic north of 42° N during boreal wintertime. In contrast, Richter and Wallace (2004) measured 3–5 times higher oceanic CH_3I with 7.1–16.4 pmol L^{-1} in boreal fall south of 15° N, and Jones et al. (2010) reported even 6 times higher concentrations (< 1.0–36.5 pmol L^{-1}) in the same region and season. Similarly to DRIVE, Jones et al. (2010) found no significant difference between open ocean and coastal regions which was ascribed to photochemical sources supported by the incubation experiments of Richter and Wallace (2004). Smythe-Wright et al. (2006) measured CH_3I as high as 45 pmol L^{-1} in the Atlantic region south of 40° N in late summer which was accompanied by high *Prochlorococcus* abundance. During DRIVE, no outstanding relationship of CH_3I with picoplankton including *Prochlorococcus* or the marker pigment divinyl chlorophyll *a* indicative of these species was found. Additionally, no correlation with diatom pigments, as suggested by Lai et al. (2011) for the production of open ocean CH_3I was observed, supporting photochemistry as important production pathway for its formation as suggested by Moore and Zafiriou (1994). The likely non-biological formation of CH_3I also leads to high saturation anomalies in open ocean surface waters. The lower saturation anomalies in the coastal zone are a result of lower temperature water upwelled to the surface diluting the more concentrated surface water (Happell and Wallace, 1996) combined with the elevated atmospheric CH_3I due to

the low MABL above the Mauritanian upwelling. However, CH_3I production may not be completely independent of biological parameters. Bell et al. (2002) suggested that organic precursors from phytoplankton production could be involved in the photochemical formation of CH_3I in the surface ocean.

Atmospheric CH_3I (0.6 to 3.3 ppt) measured during DRIVE falls well within the range of tropical Atlantic values reported by Williams et al. (2007) of 1.4 (0.6–3.0) ppt. Air mass back trajectory analysis and similar ranges of atmospheric CH_3I at open ocean station S1 and parallel at CVAO on Cape Verde hint towards open ocean air masses at both locations on 4 June (Fuhlbrügge et al., 2013). Wind speed at Cape Verde was highly variable on 6 June (Fig. 3d) leading to high variations in local sea-to-air fluxes likely causing the observed higher mean variability in atmospheric CH_3I at CVAO parallel to open ocean station S2 (Sect. 4.1.2, Fig. 3a). Atmospheric CH_3I during DRIVE at CVAO (0.7–1.8 ppt) was generally lower than what was detected by O'Brien et al. (2009) who measured on average between 1.4 and 4.6 ppt in a similar season.

Since the variability in oceanic CH_3I was not correlated to the measured biological variables and the influence from atmospheric CH_3I on oceanic concentrations was negligible, non-biological or indirect biological formation mechanisms in the surface water can be accounted for as main driver for variations of its concentration gradient across the air sea interface.

5.1.2 The relative influence of concentration gradient and wind speed on sea-to-air fluxes of CH_3I

Applying the parameterization of Nightingale et al. (2000), sea water concentrations and wind speed were almost equally important as driving factors for the CH_3I sea-to-air flux for the whole cruise region (Fig. 7) based on their similar regional variability (see the scatter in Fig. 8a and similar error bars at the plot that includes all data points in Fig. 8b). Diel variability in fluxes could be mainly ascribed to variations in oceanic CH_3I, since they were much higher than the diel variability in wind speed (Fig. 8a, b). Significant correlations of wind speed with sea-to-air fluxes of CH_3I were only found at

two 24 h-station with open ocean station S1 being the only diel stations with a very high correlation. This was caused by the general low wind speed there that consequently led to low sea-to-air fluxes despite high mean variability in CH_3I in sea surface water.

In total, sea-to-air fluxes of CH_3I encountered during DRIVE were 7.5 times lower in the open ocean and 8.7 times lower in the upwelling than fluxes calculated by Jones et al. (2010), and 3.8 times lower than fluxes reported by Richter and Wallace (2004) using similar flux parameterizations. For both other studies the higher fluxes were caused by observed higher oceanic CH_3I concentrations.

5.2 Sea-to-air fluxes of $CHBr_3$ and CH_2Br_2

5.2.1 Oceanic and atmospheric $CHBr_3$ and CH_2Br_2 as drivers of regional and diel variability of the concentration gradient

The ocean was supersaturated almost everywhere with bromocarbons during the cruise except for S2 where atmospheric $CHBr_3$ was increasing more pronounced than oceanic $CHBr_3$. The oceanic concentrations of both compounds were generally driving factors for their concentration gradients during DRIVE. Only in the open ocean atmospheric $CHBr_3$ and CH_2Br_2 reduced the sea-to-air fluxes significantly (Fig. 6) where the low oceanic concentrations were close to equilibrium with the atmosphere. The impact of oceanic concentrations on the concentration gradient increased with decreasing distance to the Mauritanian upwelling with a much more pronounced increase in oceanic $CHBr_3$ and CH_2Br_2 than in the atmosphere. The oceanic and atmospheric concentrations as well as the concentration gradients of both bromocarbons peaked simultaneously at coastal station S5. Open ocean $CHBr_3$ (1.0–3.8 pmol L^{-1}) and CH_2Br_2 (1.0–2.2 pmol L^{-1}) and increasing $CHBr_3$ (8.1–42.4 pmol L^{-1}) and CH_2Br_2 of (3.1–9.4 pmol L^{-1}) towards the coast of Mauritania during DRIVE were in good agreement to earlier studies conducted in the oligotrophic tropical and subtropical Atlantic, as in March for $CHBr_3$ (3.2–23.7 pmol L^{-1}) and for CH_2Br_2 (1.7–5.8 pmol L^{-1}) (Class and Ballschmiter, 1988), in boreal wintertime 3.2–8.0 for $CHBr_3$ and 1.0–1.8 pmol L^{-1} for

CH$_2$Br$_2$ (Schall et al., 1997) and during the same season as DRIVE with 2.1–43.6 for CHBr$_3$ and 0.7–8.7 pmol L^{-1} for CH$_2$Br$_2$ (Carpenter et al., 2009) with the highest values in the Mauritanian upwelling and close to the coast (Carpenter et al., 2009; Quack et al., 2007a). In contrast to oceanic CH$_3$I during DRIVE, oceanic CHBr$_3$ and CH$_2$Br$_2$ was elevated in the biological active regions and correlated with algal activity.

Possible biological sources during DRIVE were investigated with MLR more thoroughly: CHBr$_3$ and CH$_2$Br$_2$ showed a relationship to *Chlorophytes* and *Diatoms* while CHBr$_3$ also correlated significantly with *Cyanobacteria* and CH$_2$Br$_2$ with *Cryptophytes* (Tables 3, 5). Similar biological sources for both bromocarbons are in agreement to previous studies (Manley et al., 1992; Tokarczyk and Moore, 1994). The regional distribution of *Chlorophytes* and CHBr$_3$ and CH$_2$Br$_2$ were in best agreement to each other. *Diatoms,* although they were the dominant species in the Mauritanian upwelling and have been shown to produce halocarbons in the laboratory (Moore et al., 1996), appeared not as major contributors to bromocarbons which is in agreement to Quack et al. (2007b). Additionally, pyrophaeophorbide *a* was shown to be significant for the CHBr$_3$ distribution. This chlorophyll degradation product is specific for grazing which could lead to release of bromocarbons (Nightingale et al., 1995) produced within the algae (Moore et al., 1996).

Diel variability in the open ocean for both bromocarbons was very low and increased towards the upwelling and the coast. No relationship of halocarbons to either light, SST or salinity was found during 24 h. Elevated CHBr$_3$ and CH$_2$Br$_2$ were usually observed during evening (S3, S4 and S6) and night hours (S5). In contrast, many laboratory and field studies with both macroalgae and phytoplankton have shown maxima of CHBr$_3$ and CH$_2$Br$_2$ during the day which was attributed to light induced oxidative stress on the organisms (Ekdahl et al., 1998; Carpenter et al., 2000; Abrahamsson et al., 2004). Bromocarbon production from phytoplankton is still poorly characterized. Elevated bromocarbon production during the night could be a hint for formation during respiration in contrast to light linked production during photosynthesis (Ekdahl et al., 1998; Abrahamsson et al., 2004) or other stress factors such as grazing. Alternatively, CHBr$_3$ and

CH_2Br_2 could also be stored in the algal cells during light production and released later during the night time (Ekdahl et al., 1998) which would obscure a correlation to light in the field.

In conclusion, the regional variability of the concentration gradients of both bromocarbons was a result of the regional differences in primary production supported by their relationship to SST and phytoplankton pigment data (Sect. 4.2.3).

5.2.2 The relative influence of concentration gradient and wind speed on sea-to-air fluxes of $CHBr_3$ and CH_2Br_2

The regional distribution of sea-to-air fluxes of both bromocarbons was strongly determined by biologically produced oceanic $CHBr_3$ and CH_2Br_2. The regional variability in oceanic bromocarbons was much larger than the regional variations in wind speed (Fig. 8c–f). However, within individual stations, the variability in oceanic $CHBr_3$ and CH_2Br_2 was mostly lower than the variations in wind speed. At the open ocean stations, only very low oceanic bromocarbons were measured leading to very low concentration gradients and thus to very low sea-to-air fluxes. Here, the wind speed did not have a large impact on sea-to-air fluxes. With increasing oceanic $CHBr_3$ and CH_2Br_2 concentrations, the diel impact of changes in wind speed on the sea-to-air fluxes increased which is expressed in high correlation coefficients (Table 5, Fig. 8c and e). This effect was most pronounced for CH_2Br_2 which showed the lowest diel concentration variability of all three halocarbons (see the scatter in Fig. 8e).

Carpenter et al. (2009) derived 8.9 times higher open ocean fluxes for $CHBr_3$ and 2.4 times higher for CH_2Br_2 in comparison to this study analysing the same region and season. This resulted from larger concentration gradients due to their lower atmospheric mixing ratios using the same air–sea gas exchange parameterization. Their coastal fluxes were in the same range for both compounds as in this study caused by similar coastal concentration gradients with comparable environmental conditions.

5.3 Other impact factors on sea-to-air fluxes: MABL height and SST

Wind speed and concentration gradients are direct factors that influence sea-to-air fluxes. Some more indirect factors that could possibly impact the emissions include SST and the MABL through their intensifying or decreasing effect on the concentration gradient. Possible effects of the changes in SST on the solubility of oceanic halocarbons and therewith their concentration gradients during DRIVE were small compared to the variability in sea water concentrations. This is supported by the observed relationship of bromocarbons to increasing Chl a with decreasing SST (Fig. 2b–d). In contrast, CH_3I was independent of any physical parameters measured during DRIVE including SST (Fig. 2a and d).

The MABL height, however, has implications for both atmospheric mixing ratios of halocarbons and sea-to-air fluxes via the concentration or dilution of atmospheric halocarbons within a decreasing or increasing MABL height. In order to understand the possible effect of MABL variations, sea-to-air fluxes of all three halocarbons were calculated with the minimum and maximum atmospheric mixing ratios associated with high (from S1) and low MABL heights (from S5) to cover the range of potential fluxes (Fig. 9). A different concentration distribution can change the $CHBr_3$ and CH_2Br_2 sea-to-air fluxes on average between 19 % (S5) and 4160 % (S1) for $CHBr_3$ and between 7 % (S5) and 1337 % (S1) for CH_2Br_2 (see the lower and upper limits in Fig. 9b and c; the shading implicates the potential range). The effect on CH_3I fluxes is lower, from 1 % (S1) to 42 % (S4) (Fig. 9a) due to its high supersaturation in sea water (Fig. 4a). Atmospheric variability has a much larger potential impact on bromocarbon fluxes (Fig. 6b and c). Considering the large MABL height changes occurring within one day above coastal stations, e.g. from 100 to 350 m at S6, the effect of the entailing varying atmospheric mixing ratios on local emissions has to be taken into account when assessing halocarbon sea-to-air fluxes from coastal upwelling regions.

5.4 Oceanic influence on atmospheric mixing ratios of CH_3I, $CHBr_3$ and CH_2Br_2

5.4.1 The contribution of the oceanic emissions to the atmospheric mixing ratios

We have shown in the last sections that the sea-to-air flux of halocarbons is domi-
nated by the oceanic production and that the sea water concentrations of bromocar-
bons are increasing towards the coast. In addition, Fuhlbrügge et al. (2013) highlighted
that the MABL height, decreasing towards the coastal stations, is anticorrelated with
the atmospheric mixing ratios. In order to understand the importance for the sea-to-air
fluxes, we calculated their relative contributions to the atmospheric mixing ratios ob-
served at the individual 24 h-stations. Previous studies assigned the high $CHBr_3$ and
CH_2Br_2 mixing ratios above the coastal upwellling to air masses originating from the
North West African continent (Quack et al., 2007a) and very low atmospheric bro-
mocarbons to air masses from the northern open ocean (Carpenter et al., 2009; Lee
et al., 2010). Air masses during coastal station S5 also arrived from the northern open
ocean (Fuhlbrügge et al., 2013) which contradicts the hypothesis that high atmospheric
halocarbons could only be accounted for by continental sources. We apply a fetch of
200 km (which is the mean distance between the diel stations), sea-to-air fluxes from
Sects. 4.1.5 and 4.2.6, according wind speeds and MABL heights (Table 1). Open
ocean background values for S1 and S2 were set to 0.50 ppt for CH_3I and $CHBr_3$,
and 0.75 ppt for CH_2Br_2, while higher coastal background values of 0.75 ppt for CH_3I,
1.80 ppt for CH_2Br_2 and 3.00 ppt for $CHBr_3$ were defined for S3–S6. Here, it is note-
worthy that both the sea-to-air fluxes and the height of the MABL have numerically the
same influence on atmospheric mixing ratios since bromocarbons in the atmosphere
are within this assumption a product of both. The oceanic emissions are generally suffi-
cient to explain most of the atmospheric halocarbons (Fig. 10a–c). Oceanic halocarbon
contributions at S1–S6 (except for S5) ranged from 39 to 135 % for CH_3I, between 18
and 126 % for $CHBr_3$ and from 47 to 148 % for CH_2Br_2 with generally lowest contribu-
tions at S2 (40–69 % for CH_3I, 18–45 % for $CHBr_3$ and 47–68 % for CH_2Br_2). At S5, the

advected emissions contributed 560 (CH_3I) – 800 % ($CHBr_3$) of the observed mixing ratios. At this station high oceanic and atmospheric $CHBr_3$ and CH_2Br_2 coincided with very low MABL heights. While all mixing ratios could generally be explained with a fetch of 200 km, large scale advection seems to only account for a minor part. S5, where atmospheric halocarbons were highly overestimated with this approach, is likely a very local phenomenon that occurs when high sea-to-air fluxes, very low MABL heights and high atmospheric mixing ratios are combined. Vertical transport has been neglected in this simple approach, which may only introduce small errors since the top of the MABL was stable and isolated above the coastal stations.

While the Mauritanian upwelling has been identified to contribute to high atmospheric abundances of bromocarbons in the region, the elevated and highly variable atmospheric mixing ratios of $CHBr_3$ and CH_2Br_2 at Cape Verde were attributed to local sources. O'Brien et al. (2009) suggested high atmospheric halocarbons at CVAO originating from the coastal region off Mauritania. However, back trajectory analysis revealed air masses at CVAO originating from the open ocean during our investigation (Fuhlbrügge et al., 2013). This together with the considerably lower atmospheric mixing ratios measured at the open ocean stations (0.5–2.4 ppt for $CHBr_3$ and 0.9–1.6 ppt for CH_2Br_2) and around the upwelling contradicts upwelling originated halocarbons at Cape Verde during DRIVE. In addition, $CHBr_3$ reached its highest value of the whole campaign at CVAO. Hence, the high and variable atmospheric $CHBr_3$ and CH_2Br_2 at Cape Verde in combination with comparably variable wind speeds suggest local coastal sources for both compounds.

5.4.2 Correlations between oceanic and atmospheric $CHBr_3$ and CH_2Br_2

In contrast to Quack et al. (2007a) and Carpenter et al. (2009), atmospheric $CHBr_3$ and CH_2Br_2 regionally followed the same regional distribution as their oceanic counterparts. Water concentrations and atmospheric mixing ratios of $CHBr_3$ ($R^2 = 0.74$) and CH_2Br_2 ($R^2 = 0.85$) correlated regionally very well during DRIVE (Fig. 11a, b) which

has not been observed during other cruises in the same region (Carpenter et al., 2009; Quack et al., 2007a). This is likely caused by a combination of the stable and isolated marine boundary layer observed over the upwelling and the combined effects of air–sea exchange as slowest process (over a considerable fetch) and advection as the

5 fastest (diluting with background air) both influencing the atmospheric signals. We assume biological production of bromocarbons and mixing within the water column also as rapid processes (Ekdahl et al., 1998). Correlations within the individual 24 h-stations were only significant at open ocean station S2 for $CHBr_3$ and at coastal stations S4 and S6 for both compounds (Table 6). A diel anti-correlation of atmospheric mixing ratios

10 with water concentrations is also observed at several diel stations (S1, S2, S5, and S6). An explanation for this observation (see Table 6) between the atmospheric and oceanic concentrations on a diel scale is still lacking, since neither wind-direction, including land-sea breeze circulation (Fuhlbrügge et al., 2013), nor MABL height led to significant and clear correlations.

15 Both mean positive and negative deviations from the mean good overall regional correlation of sea water concentrations and atmospheric mixing ratios could also be observed at the individual stations. On the one hand atmospheric concentrations will increase with wind speed and increasing sea-to-air flux. On the other hand, elevated wind speeds will also trigger atmospheric dilution due to strong transport.

20 While low wind speeds in the open ocean led to a low anomaly in atmospheric mixing ratios at S1, revealing that dilution with background air appears more significant than oceanic emissions, higher wind speeds at S2 triggered average mixing ratios (Fig. 11). The increase in atmospheric mixing ratios at S2 may not only be a result of increasing sea-to-air flux and fetch but may also be partly a result of the reduction of the MABL

25 height. While coastal stations S3, S4 and S6 have similar mean $CHBr_3$ surface water concentrations, S6 showed the largest sea-to-air fluxes of these three stations due to the largest prevailing wind speeds (see Fig. 5), but on average relatively low atmospheric mixing ratios (Fig. 11a, b). We interpret this as intense transport phenomenon and possible dilution of the large sea-to-air fluxes with background air masses due to

intensifying winds and increasing MABL height. Although atmospheric mixing ratios for $CHBr_3$ and CH_2Br_2 were highest at S5, they are on average much lower as could be expected from the overall regional correlation and the large sea water concentrations (see the data points below the correlation line in Fig. 11a, b in contrast to most of the data points from other stations that are above the line). We hypothesize that the high atmospheric mixing ratios at S5, the high sea to air fluxes and low MABL height are very local phenomena with a small fetch and that regional mixing with background air masses led to the lower than average correlation of sea surface $CHBr_3$ and CH_2Br_2 and atmospheric bromocarbons. The good overall correlation between atmospheric and oceanic bromocarbons shows the dominance of sea water production for the atmosphere during our study within the known concepts of wind driven air–sea exchange and transport by wind speed and MABL variations on a regional scale.

6 Summary and conclusions

We have discussed the temporal and spatial influence of biological productivity, wind speed, MABL height and SST on oceanic emissions and atmospheric mixing ratios of halocarbons in the tropical North East Atlantic.

Oceanic CH_3I neither showed a relationship to phytoplankton pigments nor to cyanobacteria, and its distribution appeared mainly as a result of abiotic or indirect biological formation. Oceanic CH_3I was the main driver of the CH_3I concentration gradient between sea water and air. On a regional scale, neither wind speed nor oceanic CH_3I were dominating the sea-to-air flux. Diel variations in emissions were a result of varying oceanic CH_3I concentrations almost throughout the whole cruise. The regional oceanic $CHBr_3$ and CH_2Br_2 distributions and emissions were a result of biological production with no clear diurnal cycles. The variability in wind speed gained increasing impact on the diel emissions with decreasing distance to the coast. This was especially true for CH_2Br_2 because of the very small diel variability in oceanic concentrations in

Title Page

Abstract | Introduction

Conclusions | References

Tables | Figures

|◄ | ►|

◄ | ►

Back | Close

Full Screen / Esc

Printer-friendly Version

Interactive Discussion

comparison to the high diel variability in wind speed applying the flux parameterization of Nightingale et al. (2000).

MABL height is an additional factor impacting oceanic emissions through its influence on atmospheric halocarbons. Sea-to-air fluxes of CH_3I are hardly influenced by the varying MABL as a result of its high supersaturation in sea surface water. In contrast, the sea-to-air fluxes of $CHBr_3$ and CH_2Br_2 could be substantially higher or lower under different atmospheric conditions influencing their saturation anomalies. The atmospheric bromocarbons could generally be attributed to oceanic sources supported by the significant and high overall correlations of oceanic concentrations to atmospheric mixing ratios. Regional oceanic halocarbon emissions, driven by biological production can in combination with varying and low MABL heights and air mass transport explain most of the observed atmospheric halocarbons above the upwelling. Low MABL heights and high sea to air fluxes coinciding with high atmospheric mixing ratios could be a common feature in coastal upwelling systems (this study; Fuhlbrügge et al., 2013). At CVAO the high atmospheric CH_3I, $CHBr_3$ and CH_2Br_2 mixing ratios could be attributed to local coastal sources.

The temporal and spatial development of the individual impact factors (biological production, wind speed, SST and changes in atmospheric mixing ratios with MABL height) will influence the future sea-to-air fluxes and their corresponding atmospheric mixing ratios and their contribution to atmospheric chemical processes. SST and surface air temperature could play a crucial role in the future development of wind speed via the potentially increased land-sea pressure gradients, as well as in the oceanic production of halocarbons. An elevation in atmospheric CH_3I with increasing SST on a decadal scale has been shown by Yokouchi et al. (2012) in the tropical and temperate Pacific region. The potential future increase of SST in the tropical oligotrophic Atlantic (Hoerling et al., 2001) could thus lead to enhanced oceanic production of CH_3I and in combination with reduced solubility to elevated emissions of CH_3I. At the same time, the enhancement of eastern boundary upwelling systems accompanied by increasing primary production (Lachkar and Gruber, 2012) could result in higher production of oceanic bromocarbons. Combined with elevated wind speeds (Bakun, 1990), increased emissions of brominated compounds would be the

consequence. Hence, the relevance of the tropical ocean with respect to halocarbon emissions will likely increase and the influence of the diel and regional drivers may change. To better understand the current and future roles of halocarbon emissions from marine upwelling regions on global ozone changes and atmospheric chemistry, it is important to continue to better quantify the relative roles and interactions of oceanic halocarbon production, wind speed and MABL height, SST and seasonal variations, as well as other relevant forcings in coastal upwelling regions around the global ocean.

Title Page

Abstract | Introduction

Conclusions | References

Tables | Figures

|◄ | ►|

◄ | ►

Back | Close

Full Screen / Esc

Printer-friendly Version

Interactive Discussion

References

Abrahamsson, K., Lorén, A., Wulff, A., and Wangberg, S. A.: Air–sea exchange of halocarbons: the influence of diurnal and regional variations and distribution of pigments, Deep-Sea Res. Pt. II, 51, 2789–2805, doi:10.1016/j.dsr2.2004.09.005, 2004.

Aschmann, J., Sinnhuber, B.-M., Chipperfield, M. P., and Hossaini, R.: Impact of deep convection and dehydration on bromine loading in the upper troposphere and lower stratosphere, Atmos. Chem. Phys., 11, 2671–2687, doi:10.5194/acp-11-2671-2011, 2011.

Bakun, A.: Global climate change and intensification of coastal ocean upwelling, Science, 247, 198–201, doi:10.1126/science.247.4939.198, 1990.

Bange, H. W., Atlas, E. L., Bahlmann, E., Baker, A. R., Bracher, A., Cianca, A., Dengler, M., Fuhlbrügge, S., Großmann, K., Hepach, H., Lavric, J., Löscher, C., Krüger, K., Orlikowska, A., Peeken, I., Quack, B., Schafstall, J., Steinhoff, T., Williams, J., and Wittke, F.: Fs poseidon fahrtbericht/cruise report, Leibniz-Institut für Meereswissenschaften IFM-GEOMAR, Kiel, 74, 2011.

Bell, N., Hsu, L., Jacob, D. J., Schultz, M. G., Blake, D. R., Butler, J. H., King, D. B., Lobert, J. M., and Maier-Reimer, E.: Methyl iodide: atmospheric budget and use as a tracer of marine convection in global models, J. Geophys. Res.-Atmos., 107, 4340, doi:10.1029/2001jd001151, 2002.

Carpenter, L. J. and Liss, P. S.: On temperate sources of bromoform and other reactive organic bromine gases, J. Geophys. Res.-Atmos., 105, 20539–20547, 2000.

Carpenter, L. J., Malin, G., Liss, P. S., and Kupper, F. C.: Novel biogenic iodine-containing trihalomethanes and other short-lived halocarbons in the coastal east atlantic, Global Biogeochem. Cy., 14, 1191–1204, 2000.

Carpenter, L. J., Jones, C. E., Dunk, R. M., Hornsby, K. E., and Woeltjen, J.: Air-sea fluxes of biogenic bromine from the tropical and North Atlantic Ocean, Atmos. Chem. Phys., 9, 1805–1816, doi:10.5194/acp-9-1805-2009, 2009.

Class, T. and Ballschmiter, K.: Chemistry of organic traces in air viii: sources and distribution of brom- and bromochloromethanes in marine air and surfacewater of the atlantic ocean, J. Atmos. Chem., 6, 35–46, 1988.

Ekdahl, A., Pedersén, M., and Abrahamsson, K.: A study of the diurnal variation of biogenic volatile halocarbons, Mar. Chem., 63, 1–8, 1998.

Drivers of diel and regional variations

H. Hepach et al.

Title Page

Abstract	Introduction
Conclusions	References
Tables	Figures

Back | Close

Full Screen / Esc

Printer-friendly Version

Interactive Discussion

Fedoseev, A.: Geostrophic circulation of surface waters on the shelf of north-west africa, Rap. Proces., 159, 32–37, 1970.

Fuhlbrügge, S., Krüger, K., Quack, B., Atlas, E., Hepach, H., and Ziska, F.: Impact of the marine atmospheric boundary layer conditions on VSLS abundances in the eastern tropical and subtropical North Atlantic Ocean, Atmos. Chem. Phys., 13, 6345–6357, doi:10.5194/acp-13-6345-2013, 2013.

Hagen, E.: Northwest african upwelling scenario, Oceanol. Acta, 24, S113–S128, 2001.

Happell, J. D. and Wallace, D. W. R.: Methyl iodide in the greenland/norwegian seas and the tropical atlantic ocean: Evidence for photochemical production, Geophys. Res. Lett., 23, 2105–2108, doi:10.1029/96gl01764, 1996.

Hoerling, M. P., Hurrell, J. W., and Xu, T. Y.: Tropical origins for recent north atlantic climate change, Science, 292, 90–92, doi:10.1126/science.1058582, 2001.

Hossaini, R., Chipperfield, M. P., Monge-Sanz, B. M., Richards, N. A. D., Atlas, E., and Blake, D. R.: Bromoform and dibromomethane in the tropics: a 3-D model study of chemistry and transport, Atmos. Chem. Phys., 10, 719–735, doi:10.5194/acp-10-719-2010, 2010.

Hossaini, R., Chipperfield, M. P., Feng, W., Breider, T. J., Atlas, E., Montzka, S. A., Miller, B. R., Moore, F., and Elkins, J.: The contribution of natural and anthropogenic very short-lived species to stratospheric bromine, Atmos. Chem. Phys., 12, 371–380, doi:10.5194/acp-12-371-2012, 2012a.

Hossaini, R., Chipperfield, M. P., Dhomse, S., Ordonez, C., Saiz-Lopez, A., Abraham, N. L., Archibald, A., Braesicke, P., Telford, P., Warwick, N., Yang, X., and Pyle, J.: Modelling future changes to the stratospheric source gas injection of biogenic bromocarbons, Geophys. Res. Lett., 39, doi:10.1029/2012gl053401, L20813, 2012b.

Jones, C. E., Hornsby, K. E., Sommariva, R., Dunk, R. M., Von Glasow, R., McFiggans, G., and Carpenter, L. J.: Quantifying the contribution of marine organic gases to atmospheric iodine, Geophys. Res. Lett., 37, L18804, doi:10.1029/2010gl043990, 2010.

Lachkar, Z. and Gruber, N.: A comparative study of biological production in eastern boundary upwelling systems using an artificial neural network, Biogeosciences, 9, 293–308, doi:10.5194/bg-9-293-2012, 2012.

Lai, S. C., Williams, J., Arnold, S. R., Atlas, E. L., Gebhardt, S., and Hoffmann, T.: Iodine containing species in the remote marine boundary layer: a link to oceanic phytoplankton, Geophys. Res. Lett., 38, doi:10.1029/2011gl049035, L20801, 2011.

Laturnus, F.: Marine macroalgae in polar regions as natural sources for volatile organohalogens, Environ. Sci. Pollut. R., 8, 103–108, doi:10.1007/bf02987302, 2001.

Lee, J. D., McFiggans, G., Allan, J. D., Baker, A. R., Ball, S. M., Benton, A. K., Carpenter, L. J., Commane, R., Finley, B. D., Evans, M., Fuentes, E., Furneaux, K., Goddard, A., Good, N., Hamilton, J. F., Heard, D. E., Herrmann, H., Hollingsworth, A., Hopkins, J. R., Ingham, T., Irwin, M., Jones, C. E., Jones, R. L., Keene, W. C., Lawler, M. J., Lehmann, S., Lewis, A. C., Long, M. S., Mahajan, A., Methven, J., Moller, S. J., Müller, K., Müller, T., Niedermeier, N., O'Doherty, S., Oetjen, H., Plane, J. M. C., Pszenny, A. A. P., Read, K. A., Saiz-Lopez, A., Saltzman, E. S., Sander, R., von Glasow, R., Whalley, L., Wiedensohler, A., and Young, D.: Reactive Halogens in the Marine Boundary Layer (RHaMBLe): the tropical North Atlantic experiments, Atmos. Chem. Phys., 10, 1031–1055, doi:10.5194/acp-10-1031-2010, 2010.

Manley, S. L., Goodwin, K., and North, W. J.: Laboratory production of bromoform, methylene bromide, and methyl-iodide by macroalgae and distribution in nearshore southern california waters, Limnol. Oceanogr., 37, 1652–1659, 1992.

McGivern, W. S., Sorkhabi, O., Suits, A. G., Derecskei-Kovacs, A., and North, S. W.: Primary and secondary processes in the photodissociation of chbr3, J. Phys. Chem. A, 104, 10085–10091, doi:10.1021/jp0005017, 2000.

McGregor, H. V., Dima, M., Fischer, H. W., and Mulitza, S.: Rapid 20th-century increase in coastal upwelling off northwest africa, Science, 315, 637–639, doi:10.1126/science.1134839, 2007.

Minas, H. J., Codispoti, L. A., and Dugdale, R. C.: Nutrients and primary production in the upwelling region off northwest africa, Rap. Proces., 180, 148–183, 1982.

Mittelstaedt, E.: Large-scale circulation along the coast of northwest africa, Rap. Proces., 180, 50–57, 1982.

Montzka, S. A. and Reimann, S.: Ozone-depleting substances and related chemicals, in: Scientific Assessment of Ozone Depletion: 2010, Global Ozone Research and Monitoring Project, Report No. 52, World Meteorological Organization (WMO), Geneva, 108 pp., 2011.

Moore, R. M. and Zafiriou, O. C.: Photochemical production of methyl-iodide in seawater, J. Geophys. Res.-Atmos., 99, 16415–16420, doi:10.1029/94jd00786, 1994.

Moore, R. M. and Groszko, W.: Methyl iodide distribution in the ocean and fluxes to the atmosphere, J. Geophys. Res.-Oceans, 104, 11163–11171, doi:10.1029/1998jc900073, 1999.

Title Page

Abstract | Introduction

Conclusions | References

Tables | Figures

|◀ | ▶|

◀ | ▶

Back | Close

Full Screen / Esc

Printer-friendly Version

Interactive Discussion

Moore, R. M., Geen, C. E., and Tait, V. K.: Determination of henry law constants for a suite of naturally-occurring halogenated methanes in seawater, Chemosphere, 30, 1183–1191, doi:10.1016/0045-6535(95)00009-w, 1995a.

Moore, R. M., Tokarczyk, R., Tait, V. K., Poulin, M., and Geen, C. E.: Marine phytoplankton as a natural source of volatile organohalogens, in: Naturally-Produced Organohalogens, edited by: Grimvall, A., and deLeer, E. W. B., Kluwer Academic Publishers, Dordrecht, 283–294, 1995b.

Moore, R. M., Webb, M., Tokarczyk, R., and Wever, R.: Bromoperoxidase and iodoperoxidase enzymes and production of halogenated methanes in marine diatom cultures, J. Geophys. Res.-Oceans, 101, 20899–20908, doi:10.1029/96jc01248, 1996.

Nightingale, P. D., Malin, G., and Liss, P. S.: Production of chloroform and other low-molecular-weight halocarbons by some species of macroalgae, Limnol. Oceanogr., 40, 680–689, 1995.

Nightingale, P. D., Malin, G., Law, C. S., Watson, A. J., Liss, P. S., Liddicoat, M. I., Boutin, J., and Upstill-Goddard, R. C.: In situ evaluation of air–sea gas exchange parameterizations using novel conservative and volatile tracers, Global Biogeochem. Cy., 14, 373–387, doi:10.1029/1999gb900091, 2000.

O'Brien, L. M., Harris, N. R. P., Robinson, A. D., Gostlow, B., Warwick, N., Yang, X., and Pyle, J. A.: Bromocarbons in the tropical marine boundary layer at the Cape Verde Observatory – measurements and modelling, Atmos. Chem. Phys., 9, 9083–9099, doi:10.5194/acp-9-9083-2009, 2009.

O'Dowd, C. D., Jimenez, J. L., Bahreini, R., Flagan, R. C., Seinfeld, J. H., Hameri, K., Pirjola, L., Kulmala, M., Jennings, S. G., and Hoffmann, T.: Marine aerosol formation from biogenic iodine emissions, Nature, 417, 632–636, doi:10.1038/nature00775, 2002.

Pyle, J. A., Warwick, N., Yang, X., Young, P. J., and Zeng, G.: Climate/chemistry feedbacks and biogenic emissions, Philos. T. R. Soc. A, 365, 1727–1740, doi:10.1098/rsta.2007.2041, 2007.

Quack, B. and Wallace, D. W. R.: Air-sea flux of bromoform: controls, rates, and implications, Global Biogeochem. Cy., 17, 1023, doi:10.1029/2002gb001890, 2003.

Quack, B., Atlas, E., Petrick, G., Stroud, V., Schauffler, S., and Wallace, D. W. R.: Oceanic bromoform sources for the tropical atmosphere, Geophys. Res. Lett., 31, L23s05, doi:10.1029/2004gl020597, 2004.

Quack, B., Atlas, E., Petrick, G., and Wallace, D. W. R.: Bromoform and dibromomethane above the mauritanian upwelling: atmospheric distributions and oceanic emissions, J. Geophys. Res.-Atmos., 112, D09312, doi:10.1029/2006jd007614, 2007a.

Quack, B., Peeken, I., Petrick, G., and Nachtigall, K.: Oceanic distribution and sources of bromoform and dibromomethane in the mauritanian upwelling, J. Geophys. Res.-Oceans, 112, C10006, doi:10.1029/2006jc003803, 2007b.

Richter, U. and Wallace, D. W. R.: Production of methyl iodide in the tropical atlantic ocean, Geophys. Res. Lett., 31, L23s03, doi:10.1029/2004gl020779, 2004.

Saiz-Lopez, A., Plane, J. M. C., Baker, A. R., Carpenter, L. J., von Glasow, R., Martin, J. C. G., McFiggans, G., and Saunders, R. W.: Atmospheric chemistry of iodine, Chem. Rev., 112, 1773–1804, doi:10.1021/cr200029u, 2012.

Salawitch, R. J., Weisenstein, D. K., Kovalenko, L. J., Sioris, C. E., Wennberg, P. O., Chance, K., Ko, M. K. W., and McLinden, C. A.: Sensitivity of ozone to bromine in the lower stratosphere, Geophys. Res. Lett., 32, L05811, doi:10.1029/2004gl021504, 2005.

Schall, C., Heumann, K. G., and Kirst, G. O.: Biogenic volatile organoiodine and organobromine hydrocarbons in the atlantic ocean from 42° N to 72° S, Fresenius, J. Anal. Chem., 359, 298–305, 1997.

Schauffler, S. M., Atlas, E. L., Blake, D. R., Flocke, F., Lueb, R. A., Lee-Taylor, J. M., Stroud, V., and Travnicek, W.: Distributions of brominated organic compounds in the troposphere and lower stratosphere, J. Geophys. Res.-Atmos., 104, 21513–21535, 1999.

Smythe-Wright, D., Boswell, S. M., Breithaupt, P., Davidson, R. D., Dimmer, C. H., and Diaz, L. B. E.: Methyl iodide production in the ocean: Implications for climate change, Global Biogeochem. Cy., 20, Gb3003, doi:10.1029/2005gb002642, 2006.

Solomon, S., Garcia, R. R., and Ravishankara, A. R.: On the role of iodine in ozone depletion, J. Geophys. Res.-Atmos., 99, 20491–20499, doi:10.1029/94jd02028, 1994.

Taylor, B. B., Torrecilla, E., Bernhardt, A., Taylor, M. H., Peeken, I., Röttgers, R., Piera, J., and Bracher, A.: Bio-optical provinces in the eastern Atlantic Ocean and their biogeographical relevance, Biogeosciences, 8, 3609–3629, doi:10.5194/bg-8-3609-2011, 2011.

Tegtmeier, S., Krüger, K., Quack, B., Atlas, E. L., Pisso, I., Stohl, A., and Yang, X.: Emission and transport of bromocarbons: from the West Pacific ocean into the stratosphere, Atmos. Chem. Phys., 12, 10633–10648, doi:10.5194/acp-12-10633-2012, 2012.

Tegtmeier, S., Krüger, K., Quack, B., Atlas, E., Blake, D. R., Boenisch, H., Engel, A., Hepach, H., Hossaini, R., Navarro, M. A., Raimund, S., Sala, S., Shi, Q., and Ziska, F.: The contribution

of oceanic methyl iodide to stratospheric iodine, Atmos. Chem. Phys. Discuss., 13, 11427–11471, doi:10.5194/acpd-13-11427-2013, 2013.

Tokarczyk, R. and Moore, R. M.: Production of volatile organohalogens by phytoplankton cultures, Geophys. Res. Lett., 21, 285–288, 1994.

Tomczak, M.: The distribution of water masses at the surface as derived from t-s diagram analysis in the cineca area, Rap. Proces., 180, 48–49, 1982.

Tomczak, M. and Godfrey, J. S.: Regional Oceanography: an Introduction, 2 edn., Daya Publishing House, Delhi, 2005.

Tran, S., Bonsang, B., Gros, V., Peeken, I., Sarda-Esteve, R., Bernhardt, A., and Belviso, S.: A survey of carbon monoxide and non-methane hydrocarbons in the Arctic Ocean during summer 2010, Biogeosciences, 10, 1909–1935, doi:10.5194/bg-10-1909-2013, 2013.

Williams, J., Gros, V., Atlas, E., Maciejczyk, K., Batsaikhan, A., Scholer, H. F., Forster, C., Quack, B., Yassaa, N., Sander, R., and Van Dingenen, R.: Possible evidence for a connection between methyl iodide emissions and saharan dust, J. Geophys. Res.-Atmos., 112, doi:10.1029/2005jd006702, D07302, 2007.

Tsuchiya, M., Talley, L. D., and McCartney, M. S.: An eastern atlantic section from iceland southward across the equator, Deep-Sea Res., 39, 1885–1917, doi:10.1016/0198-0149(92)90004-d, 1992.

Yokouchi, Y., Osada, K., Wada, M., Hasebe, F., Agama, M., Murakami, R., Mukai, H., Nojiri, Y., Inuzuka, Y., Toom-Sauntry, D., and Fraser, P.: Global distribution and seasonal concentration change of methyl iodide in the atmosphere, J. Geophys. Res.-Atmos., 113, doi:10.1029/2008jd009861, D18311, 2008.

Yokouchi, Y., Nojiri, Y., Toom-Sauntry, D., Fraser, P., Inuzuka, Y., Tanimoto, H., Nara, H., Murakami, R., and Mukai, H.: Long-term variation of atmospheric methyl iodide and its link to global environmental change, Geophys. Res. Lett., 39, doi:10.1029/2012gl053695, L23805, 2012.

Ziska, F., Quack, B., Abrahamsson, K., Archer, S. D., Atlas, E., Bell, T., Butler, J. H., Carpenter, L. J., Jones, C. E., Harris, N. R. P., Hepach, H., Heumann, K. G., Hughes, C., Kuss, J., Krüger, K., Liss, P., Moore, R. M., Orlikowska, A., Raimund, S., Reeves, C. E., Reifenhäuser, W., Robinson, A. D., Schall, C., Tanhua, T., Tegtmeier, S., Turner, S., Wang, L., Wallace, D., Williams, J., Yamamoto, H., Yvon-Lewis, S., and Yokouchi, Y.: Global sea-to-air flux climatology for bromoform, dibromomethane and methyl iodide, Atmos. Chem. Phys. Discuss., 13, 5601–5648, doi:10.5194/acpd-13-5601-2013, 2013.

Title Page

Abstract | Introduction

Conclusions | References

Tables | Figures

◀◀ | ▶▶

◀ | ▶

Back | Close

Full Screen / Esc

Printer-friendly Version

Interactive Discussion

Table 1. Means and ranges (minimum–maximum) of ambient parameters (SST, salinity, Chl *a*, wind speed, MABL height) during DRIVE for open ocean stations S1–S2 and coastal stations S3–S6.

Parameter	Unit	S1 17.6° N and 24.3° W	S2 18.0° N and 21.0° W	S3 18.0° N and 18.0° W	S4 18.5° N and 16.5° W	S5 19.0° N and 16.6° W	S6 20.0° N and 17.3° W
SST	°C	24.5 (24.4–24.7)	23.2 (23.0–23.6)	21.7 (21.6–21.8)	23.3 (23.1–23.4)	20.4 (20.2–21.0)	18.6 (18.4–18.7)
Salinity		36.7 (36.7–36.7)	36.4 (36.4–36.5)	35.9 (35.9–35.9)	35.9 (35.9–35.9)	35.8 (35.8–35.8)	35.9 (35.8–35.9)
Chl *a*	$\mu g\,L^{-1}$	0.05 (0–0.08)	0.30 (0.10–0.43)	1.00 (0.58–1.79)	1.63 (0.81–3.01)	4.50 (1.69–8.12)	4.80 (7.40–6.70)
Wind speed	$m\,s^{-1}$	4.6 (2.0–7.1)	11.0 (7.8–14.8)	6.0 (3.9–9.0)	9.7 (6.7–12.9)	8.9 (4.3–13.7)	11.0 (6.8–14.2)
MABL height	m	950 (850–1100)	540 (400–700)	290 (200–400)	120 (50–200)	25 (surface–100)	190 (100–350)

Table 2. Results of halocarbon measurements (water and air) and calculations (saturation anomalies and sea-to-air fluxes) for all six diel stations and parallel air sampling at CVAO.

Compound	Parameter	Unit	S1 17.6° N and 24.3° W	S2 18.0° N and 21.0° W	S3 18.0° N and 18.0° W	S4 18.5° N and 16.5° W	S5 19.0° N and 16.6° W	S6 20.0° N and 17.3° W
CH_3I	Water	$pmol\,L^{-1}$	3.0 (1.7–5.4)	1.8 (0.4–3.9)	1.2 (0.2–2.1)	1.6 (0.6–3.4)	2.2 (0.1–4.5)	2.0 (0.8–3.5)
	Air	ppt	0.7 (0.6–1.0)	1.1 (1.0–1.3)	1.0 (0.9–1.1)	1.6 (1.1–2.7)	2.3 (1.4–3.3)	1.3 (1.1–2.7)
	CVAO air	ppt	0.9 (0.7–1.0)	1.4 (1.1–1.8)	–	–	–	–
	Saturation anomaly	%	2606.3 (1321.1–4597.1)	870.2 (99.4–2243.7)	532.2 (−8.5–967.1)	445.6 (90.8–1167.4)	410.8 (−65.8–928.7)	672.1 (210.1–1242.3)
	Sea-to-air flux	$pmol\,m^{-2}\,h^{-1}$	158.3 (59.3–330.4)	372.6 (39.6–941.6)	79.0 (−1.7–212.2)	227.7 (61.4–500.5)	259.6 (−64.6–871.6)	382.5 (106.1–837.9)
$CHBr_3$	Water	$pmol\,L^{-1}$	1.2 (1.0–1.6)	3.0 (1.9–3.8)	16.2 (11.3–25.5)	11.9 (8.1–14.7)	30.6 (26.1–42.4)	15.3 (12.8–17.5)
	Air	ppt	0.6 (0.5–0.8)	1.8 (1.2–2.4)	5.3 (4.2–6.1)	5.3 (4.2–6.6)	7.0 (5.4–8.9)	4.9 (4.1–6.0)
	CVAO air	ppt	6.7 (2.3–12.8)	6.8 (3.7–12.8)	–	–	–	–
	Saturation anomaly	%	39.6 (−14.7–79.3)	17.7 (−40.3–97.3)	80.6 (43.0–212.7)	46.1 (5.2–94.4)	148.0 (69.4–243.1)	59.4 (5.4–105.5)
	Sea-to-air flux	$pmol\,m^{-2}\,h^{-1}$	15.5 (−8.5–45.0)	65.6 (−273.4–426.7)	489.1 (241.4–1610.9)	611.7 (41.7–1333.8)	2423.0 (1063.3–6068.9)	1098.2 (77.8–2360.2)
CH_2Br_2	Water	$pmol\,L^{-1}$	1.2 (1.0–1.3)	1.9 (1.5–2.2)	4.0 (3.1–4.9)	5.4 (4.1–6.1)	8.8 (8.1–9.4)	5.1 (4.6–5.8)
	Air	ppt	1.0 (0.9–1.1)	1.4 (1.1–1.6)	2.2 (2.0–2.4)	2.4 (2.0–2.9)	2.8 (2.5–3.1)	2.1 (1.9–2.3)
	CVAO air	ppt	1.4 (1.1–2.1)	1.5 (1.2–2.0)	–	–	–	–
	Saturation anomaly	%	24.7 (3.4–43.2)	37.7 (4.1–72.2)	64.7 (30.9–111.5)	122.0 (82.7–165.0)	169.0 (131.8–204.3)	86.1 (70.1–110.6)
	Sea-to-air flux	$pmol\,m^{-2}\,h^{-1}$	10.6 (1.8–27.9)	118.5 (14.5–214.3)	115.7 (50.0–260.3)	511.8 (207.9–801.0)	815.4 (285.6–1429.4)	470.4 (295.5–671.6)

Table 3. Correlation coefficients R^2 of halocarbons to nano- and picoplankton abundances as well as to phytoplankton pigment data (MLR – Multiple Linear Regression). The correlations to Prochlorococcchus are all significant on the $p < 0.05$ level. Negative correlations are printed in bold.

		n	CH_3I	$CHBr_3$	CH_2Br_2
Nano- and picoplankton	Prochlorococcus	72	0.10	**0.39**	**0.26**
	Others	72	< 0.08	< 0.09	< 0.10
Phyotplankton pigments	Chl a	61	0.00	0.38	0.49
	MLR	61	None	0.79	0.77

Title Page

Abstract | Introduction

Conclusions | References

Tables | Figures

|◄ | ►|

◄ | ►

Back | Close

Full Screen / Esc

Table 4. Correlation coefficients for water concentrations of halocarbons and wind speed with sea-to-air fluxes of halocarbons for the whole cruise and for the individual stations. Coefficients printed in bold represent significant correlations with $p < 0.05$.

Station	R^2 of	with F of			n
		CH_3I	$CHBr_3$	CH_2Br_2	
Whole cruise	Water concentration	**0.37**	**0.68**	**0.71**	109
	Wind speed	**0.24**	**0.14**	**0.29**	
S1 (17.6° N and 24.3° W)	Water concentration	**0.24**	**0.66**	**0.35**	18
	Wind speed	**0.73**	**0.28**	0.21	
S2 (18.0° N and 21.0° W)	Water concentration	**0.89**	**0.78**	**0.64**	19
	Wind speed	0.00	0.00	0.15	
S3 (18.0° N and 18.0° W)	Water concentration	**0.67**	**0.66**	**0.42**	17
	Wind speed	**0.24**	0.21	**0.56**	
S4 (18.5° N and 16.5° W)	Water concentration	**0.91**	**0.60**	**0.53**	17
	Wind speed	0.02	**0.67**	**0.93**	
S5 (19.0° N and 16.6° W)	Water concentration	**0.57**	**0.34**	0.09	18
	Wind speed	0.02	**0.55**	**0.95**	
S6 (20.0° N and 17.3° W)	Water concentration	**0.79**	**0.70**	0.00	20
	Wind speed	0.06	**0.82**	**0.78**	

Table 5. Phytoplankton pigments that were found to be significant at $p < 0.05$ and what they are indicative for.

Pigment	Indicative for	CHBr$_3$	CH$_2$Br$_2$
Chlorophyll *b*	Chlorophytes	x	x
Chlorophyll *c3*	Haptophytes	x	
Fucoxanthin	Diatoms	x	x
Diatoxanthin		x	
Zeaxanthin	Cyanobacteria	x	
α-carotene	Cryptophytes		x
Alloxanthin			x
Pyrophaephorbide a	Grazing	x	

Table 6. Correlation coefficients R^2 and number of data points n of oceanic vs. atmospheric bromocarbons for the whole cruise and each individual station. Bold numbers indicate significant correlations with $p < 0.05$. Italic numbers mark negative correlations.

	Whole cruise	S1 (17.6° N and 24.3° W)	S2 (18.0° N and 21.0° W)	S3 (18.0° N and 18.0° W)	S4 (18.5° N and 16.5° W)	S5 (19.0° N and 16.6° W)	S6 (20.0° N and 17.3° W)
$CHBr_3$	**0.74**	*0.01*	***0.52***	0.01	**0.45**	*0.05*	***0.20***
CH_2Br_2	**0.85**	*0.19*	*0.09*	0.01	**0.40**	*0.18*	**0.28**
n	109	18	19	17	17	18	20
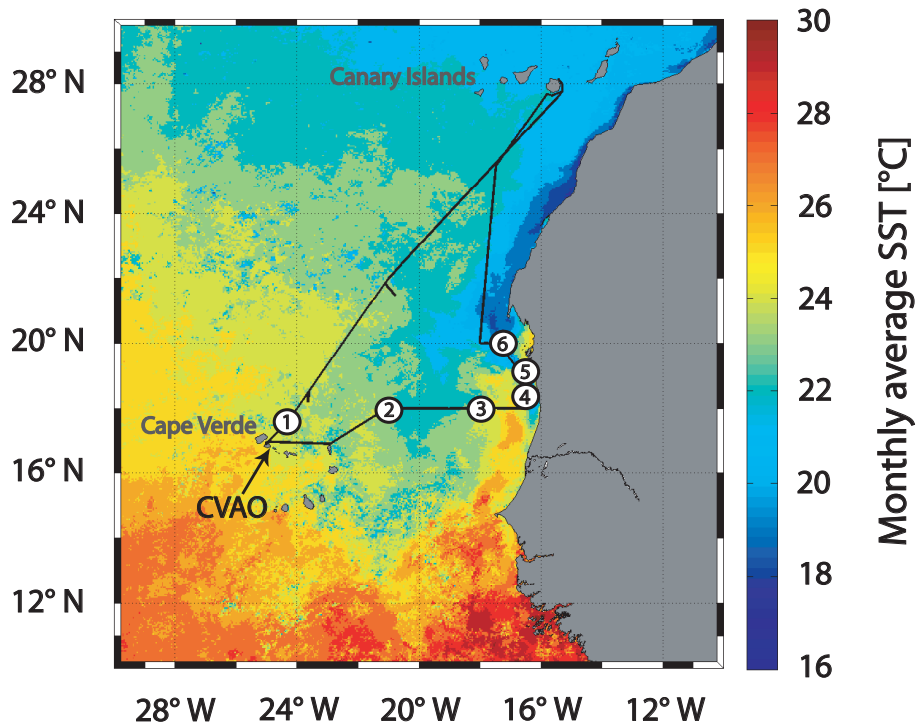
Fig. 1. Cruise track (black line) during DRIVE on SST derived from the monthly composite of June 2010 of MODIS-Aqua level 3 data. White circles with black numbers indicate 24 h-stations. Also marked is the location of the CVAO (Cape Verde Atmospheric Observatory).
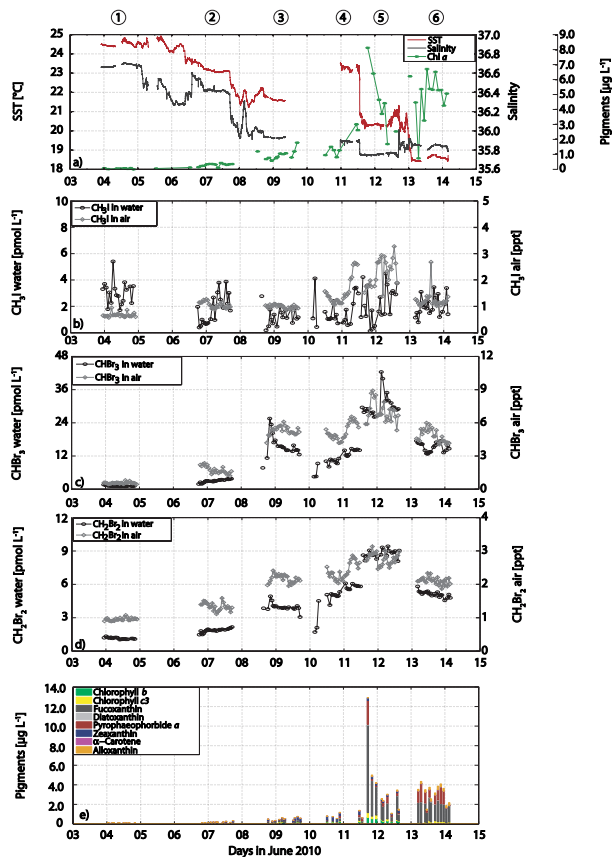
Fig. 2. SST, salinity and Chl *a* **(a)** along with halocarbon concentrations in water and atmospheric mixing ratios of CH$_3$I **(b)**, CHBr$_3$ **(c)** and CH$_2$Br$_2$ **(d)** and pigments significant for the regional distribution of CHBr$_3$ and CH$_2$Br$_2$ **(e)** during the DRIVE campaign.

Title Page

Abstract | Introduction

Conclusions | References

Tables | Figures

|◄ | ►|

◄ | ►

Back | Close

Full Screen / Esc

Printer-friendly Version

Interactive Discussion
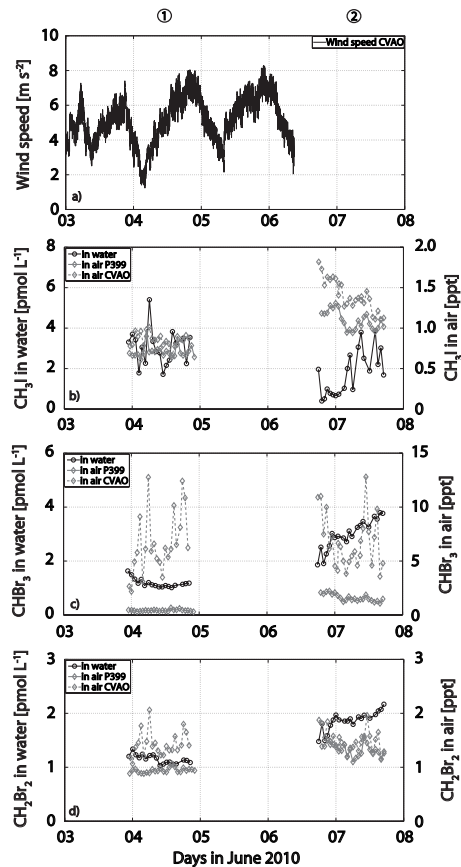
Fig. 3. Open ocean surface water and atmospheric halocarbons during stations S1 and S2 and atmospheric halocarbons measured parallel at CVAO as well as wind speed (wind speed in **(a)**, CH_3I in **(b)**, $CHBr_3$ in **(c)**, and CH_2Br_2 in **(d)**). Wind speed data for 7 and 8 June in 2010 was not available.
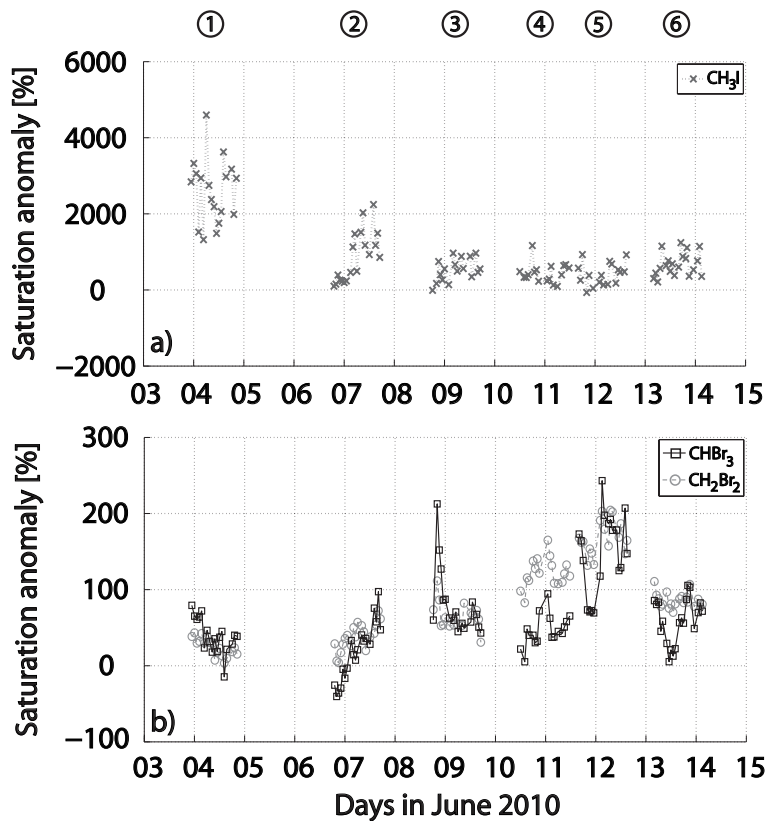
Fig. 4. Saturation anomalies of CH_3I **(a)** and $CHBr_3$ and CH_2Br_2 **(b)** throughout the RV *Poseidon* cruise.

Title Page

Abstract | Introduction

Conclusions | References

Tables | Figures

|◄ | ►|

◄ | ►

Back | Close

Full Screen / Esc

Printer-friendly Version

Interactive Discussion
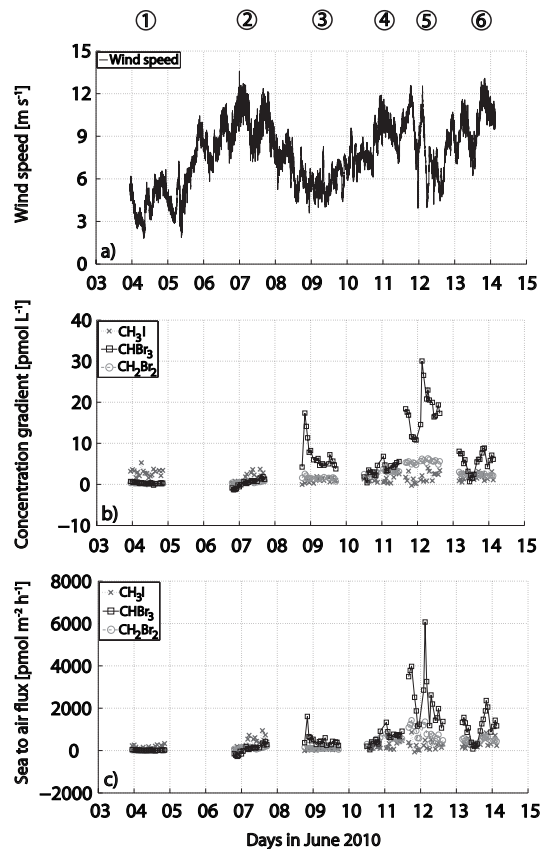
Fig. 5. Wind speed **(a)**, concentration gradients **(b)** and sea-to-air fluxes **(c)** of CH_3I, $CHBr_3$ and CH_2Br_2 during DRIVE.
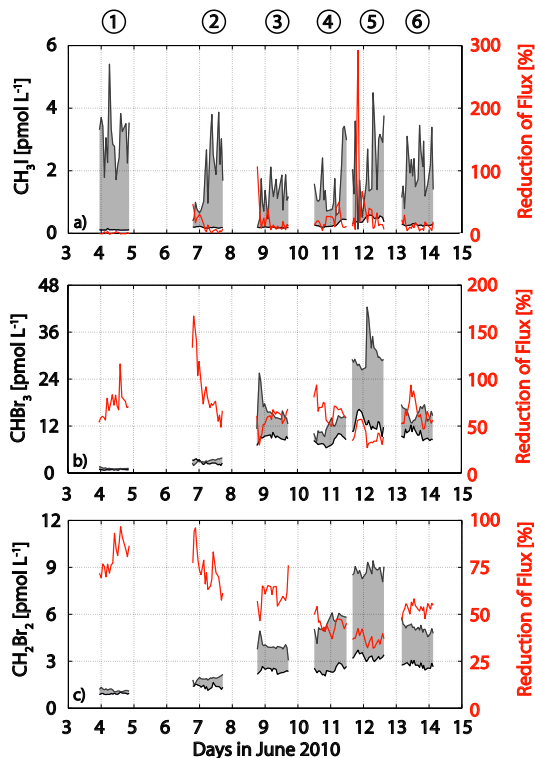
Fig. 6. Influence of atmospheric mixing ratios on the amount of oceanic halocarbons emitted for CH_3I **(a)**, $CHBr_3$ **(b)**, and CH_2Br_2 **(c)**. Oceanic concentrations are plotted in grey (left axis), the equilibrium concentration is delineated in black, and the concentration gradient is shaded in grey. The percentaged reduction of the concentration gradient by the equilibrium concentration (flux reducing effect) derived from the atmospheric measurements (equilibrium concentration in percent in relation to the water concentrations) is shown in red (right axis).

Title Page

Abstract | Introduction

Conclusions | References

Tables | Figures

|◀ | ▶|

◀ | ▶

Back | Close

Full Screen / Esc
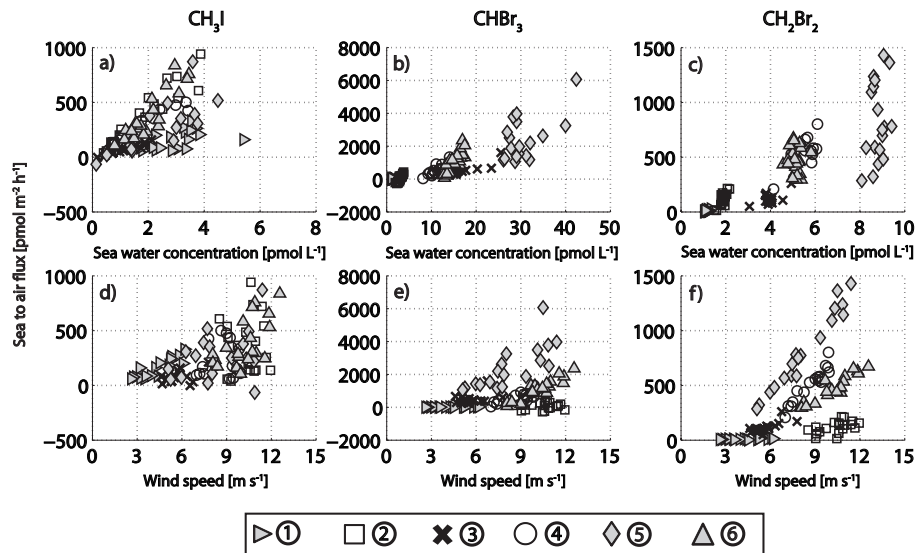
Fig. 7. Sea-to-air fluxes vs. sea water concentrations of CH_3I **(a)**, $CHBr_3$ **(b)** and CH_2Br_2 **(c)** and wind speed **(d–f)** during DRIVE.
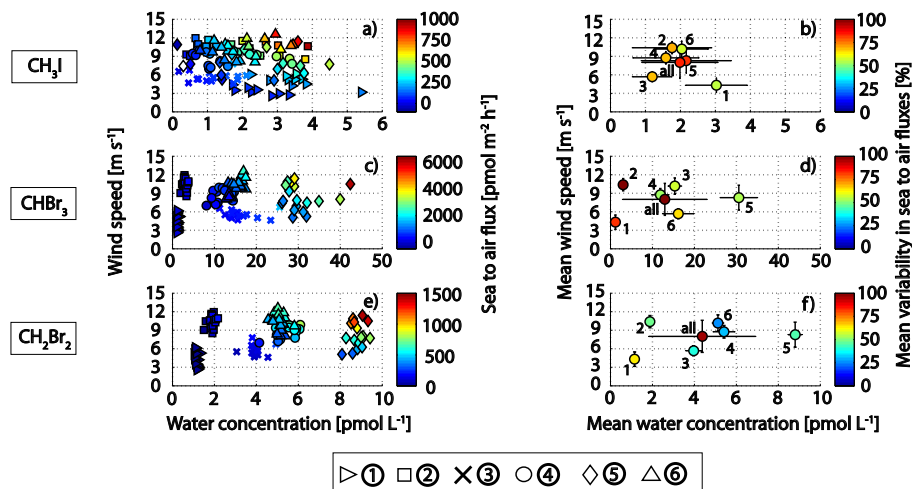
Fig. 8. Left side – wind speed vs. CH_3I **(a)**, $CHBr_3$ **(c)** and CH_2Br_2 **(e)** water concentrations. Symbols are filled according to their sea-to-air flux (see color bars). Right side – mean wind speed vs. mean CH_3I **(b)**, $CHBr_3$ **(d)** and CH_2Br_2 **(f)** water concentrations with their standard deviations which is expressed in error bars (horizontal for water concentrations and vertical for wind speed) for each diel station (S1–S6) and for all stations together. Symbols are filled with the relative standard deviations of the sea-to-air fluxes (see color bars).
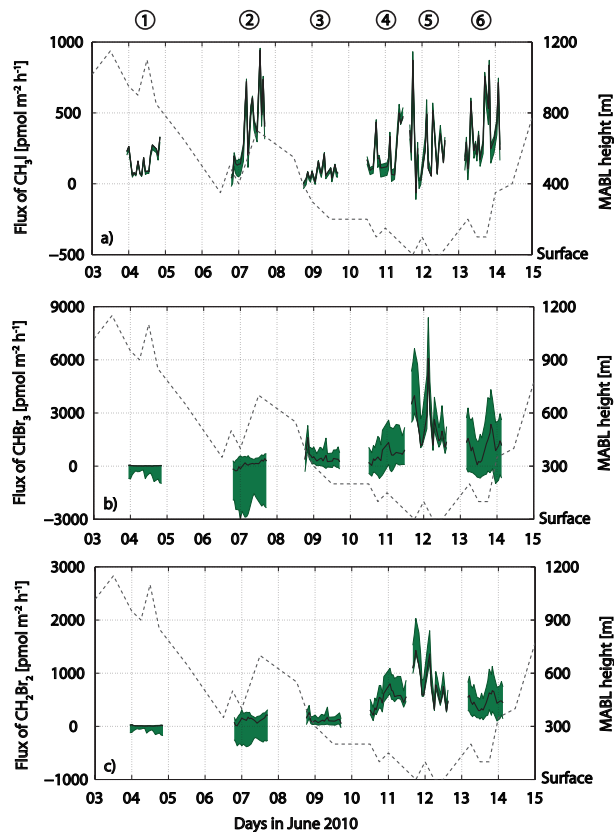
Fig. 9. Sea-to-air fluxes for CH_3I **(a)**, $CHBr_3$ **(b)** and CH_2Br_2 **(c)** during DRIVE and the MABL height, determined by Fuhlbrügge et al. (2013) as the dashed grey line are shown on the right side. The upper and lower value of potential sea-to-air fluxes assuming the lowest MABL (lower range, 3.0 ppt for CH_3I, 3.1 ppt for CH_2Br_2 and 8.9 ppt for $CHBr_3$) and the highest MABL (upper range, 0.6 ppt for CH_3I, 0.9 ppt for CH_2Br_2 and 0.5 ppt for $CHBr_3$) valid for the whole region are shaded in green.

Title Page

Abstract | Introduction

Conclusions | References

Tables | Figures

|◄ | ►|

◄ | ►

Back | Close

Full Screen / Esc

Printer-friendly Version
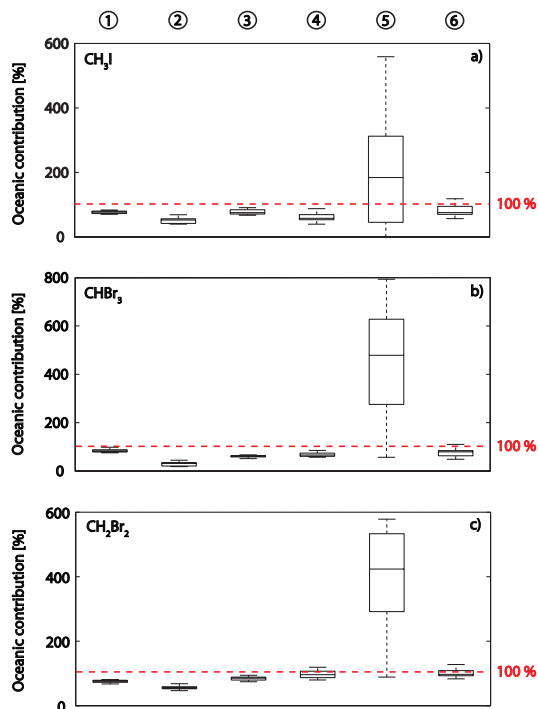
Interactive Discussion

Fig. 10. Oceanic contributions to atmospheric halocarbons assuming a mean distance of 200 km, mean wind speeds, mean sea-to-air fluxes and background mixing ratios for the open ocean ($CH_3I = 0.50$ ppt, $CHBr_3 = 0.50$ ppt, $CH_2Br_2 = 0.75$ ppt) and the coastal region ($CH_3I = 0.75$ ppt, $CHBr_3 = 3.00$ ppt, $CH_2Br_2 = 1.80$ ppt), and the MABL heights determined by Fuhlbrügge et al. (2013) at every measurement point for CH_3I **(a)**, for $CHBr_3$ **(b)** and for CH_2Br_2 **(c)**, outliers are excluded. The red dashed line marks 100 % in every plot.

Title Page

Abstract | Introduction

Conclusions | References

Tables | Figures

|◄ | ►|

◄ | ►

Back | Close

Full Screen / Esc

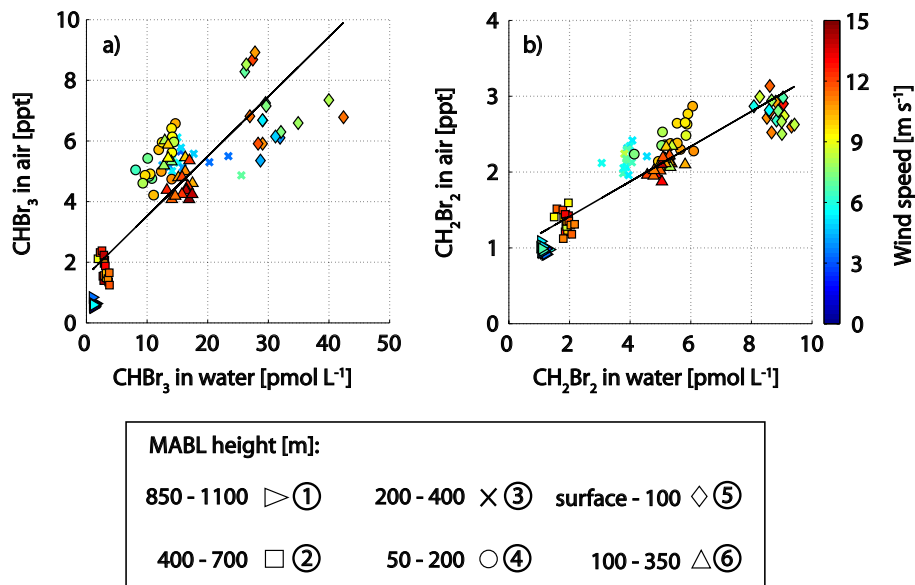Printer-friendly Version

Interactive Discussion

Fig. 11. Correlations of oceanic vs. atmospheric halocarbons ($CHBr_3$ in **(a)** and CH_2Br_2 in **(b)**) filled with wind speed (see color coding). The black line indicates the regression line for the whole cruise. For the individual correlation coefficients see Table 6.